Age-dependent differential iron deficiency responses of rosette leaves during reproductive stages in *Arabidopsis thaliana*

Short title: **Differential iron deficiency responses of rosette leaves during reproduction**

Mary Ngigi[1,2], Mather Khan[1,2,3], Ricarda Remus[1], Shishir K Gupta[1,2, §], Petra Bauer[1,2]

[1]Institute of Botany, Heinrich-Heine-University, 40225 Düsseldorf, Germany

[2]Cluster of Excellence on Plant Science (CEPLAS), Heinrich-Heine-University, 40225 Düsseldorf, Germany

[3] Division of Plant Science & Technology, C.S. Bond Life Sciences Center, University of Missouri, Columbia, MO 65211, USA

[§]Department of Data Sciences, Centre of Biomedical Research, Sanjay Gandhi Post-Graduate Institute of Medical Sciences Campus, Raebareli Road, Lucknow, 226014, India

ORCID IDs

Mary Ngigi	0000-0001-7307-9563
Mather Khan	0000-0002-4141-3106
Ricarda Remus	0009-0003-0647-7934
Shishir K Gupta	0000-0002-2335-1597
Petra Bauer	0000-0002-0404-4532

Email addresses

Mary Ngigi - Mary.Ngigi@hhu.de

Mather Khan - khanma@missouri.edu

Ricarda Remus - rirem100@uni-duesseldorf.de

Shishir K Gupta - shishir.bioinfo@gmail.com

Petra Bauer - Petra.Bauer@hhu.de

* Corresponding author: Petra Bauer (Petra.Bauer@hhu.de)

The author responsible for distribution of materials integral to the findings presented in this article in accordance with the policy described in the Instructions for Authors (https://academic.oup.com/plcell/pages/General-Instructions) is Petra Bauer (Petra.Bauer@hhu.de).

One-sentence summary:

This study explores reproductive stage-dependent responses of rosette leaves to iron availability, revealing distinct growth, elemental contents, and gene expression patterns between young and old leaves and stages.

Major findings:

- Young leaves but not old leaves exhibited rapid growth inhibition and chlorosis under -Fe conditions.
- Significant differences in gene expression and ionomics profile were observed between old and young leaves.
- Contrasts were noted between the early reproductive stages (RS, BS) and the late ones (FS, MS).
- Correlations between ionomics profiles and gene expression indicated a complex interaction.

Key words

Copper, Gene co-expression, Iron, leaf signaling, manganese, old leaves, reproduction, rosette leaves, young leaves, zinc

Abstract

Iron is essential for plant development throughout the life cycle. When plants lack the crucial micronutrient iron (Fe), they develop interveinal leaf chlorosis and stunted growth. To cope with this, they adjust gene expression and manage Fe and other metal ions accordingly. Rosette leaves may act as Fe

sources and Fe sinks. Little is known about the dynamics of Fe deficiency (-Fe) responses in the *Arabidopsis thaliana* rosette leaves during the reproductive stages.

We studied the dynamics of Fe-dependent responses at four consecutive reproductive stages (rosette, bolting, flowering, mature silique stages, hereby named RS, BS, FS, MS). We examined the growth of rosette leaves, elemental contents and gene expression patterns of Fe homeostasis genes belonging to differently regulated groups. We determined individual leaf sizes during seven days of +Fe and -Fe treatment at the RS.

Young leaves responded rapidly to -Fe with growth inhibition and yellowing. Old and young leaves differed in gene expression patterns and elemental contents. Differences were also noted between the early and late reproductive stages (primarily RS and BS versus MS) and correlations between ionomic contents and gene expression were detected. Although all leaves had induced Fe recycling genes at -Fe, the expression patterns of "High Fe" and other Fe marker genes together with elemental contents indicate that old leaves at the RS and BS might serve as Fe sources, while young leaves might be Fe sinks at +Fe.

Our findings highlight a developmental stage-dependent modulation of +Fe and -Fe responses in leaves. We discuss possible leaf signaling mechanisms accounting for the distinct responses between old and young leaves. This insight is informative for iron management in crops.

Introduction

Iron (Fe) is a vital micronutrient for all organisms. In plants, Fe is central for the many fundamental Fe-requiring metabolic processes like photosynthesis, nutrient assimilation, chlorophyll synthesis, and oxidative stress defense (Briat et al., 2007; Jeong & Guerinot, 2009). Fe is often not bioavailable in soil and limiting during plant growth, requiring acclimation of plant Fe physiology. The complexities of iron homeostasis and networks of Fe-related cell physiological functions can be unraveled by exposing plants to Fe deficiency (-Fe) and recording growth data, ionomics profiles, and Fe-related gene expression patterns. Understanding Fe-regulatory pathways paves the way for innovations in translational plant biotechnology, such as to generate biofortified Fe-rich crops for food nutritional security that are suited for sustainable agroecological practices.

Arabidopsis thaliana has greatly served as a model species to generate knowledge about the regulation and genetic networks that steer the ways how Fe is acquired and allocated in plants (Sági-Kazár

et al., 2022). Yet, there are some gaps in our understanding. Many studies focused on investigating the roles of Fe-regulatory genes, particularly in young seedlings and during the vegetative growth phase (Khan et al., 2018; Nguyen et al., 2022). The few studies, that examined Fe management during reproduction, concluded that *de novo* Fe uptake and Fe recycling are important to compensate for a lack of Fe, and that rosette leaves may act as Fe reserves that possibly supply Fe to newly developing organs through remobilization mechanisms (Pottier et al., 2019; Schuler et al., 2012; Waters & Grusak, 2008). Yet, to our knowledge, a detailed and systematic study that investigates how different rosette leaves of Arabidopsis respond to -Fe cues during the early and late reproductive stages is missing.

During the reproductive stages, the rosette leaves can be classified into old and young leaves, distinguishing them based on their age whereby first true leaves are fully matured at the onset of reproduction, while the later developed leaves continuously grow and expand until late reproductive stages. Old and young leaf types differ in morphology and size, and hints are available that they also show variation in the regulation of Fe homeostasis (Nguyen et al., 2022; Schuler et al., 2012). Better understanding how different types of leaves manage Fe and Fe-related gene expression will provide new insights into leaf Fe signaling in Arabidopsis. Numerous mutants and tools are available in *A. thaliana*, that can be leveraged for further studies to better understand the genetic mechanisms directing Fe physiology during reproduction.

Gene co-expression analysis is a powerful tool to decipher Fe-regulatory networks, cell functions, and pathways for Fe management at Fe sufficiency (+Fe) and Fe deficiency (-Fe) conditions (Ivanov et al., 2012; Schwarz & Bauer, 2020). Co-expression indicates that different genes interact so that their collective expression leads to specific cellular and physiological outcomes being controlled by similar stimuli such as +Fe or -Fe. Of particular interest, the similar expression patterns of co-expressed -Fe-regulated genes across different conditions, time points, or tissues, indicate that they are most likely regulated by the same group of transcription factors and involved in related Fe regulatory processes (Schwarz & Bauer, 2020). Analyzing -Fe-induced co-expressed genes has helped to understand the complexities of Fe-regulatory systems. The Fe deficiency-induced co-expressed genes are divided into sub-co-expression networks, that reflect the division into different Fe-related functions (Ivanov et al., 2012; Schwarz & Bauer, 2020). One subset of genes or co-expression cluster induced in response to -Fe in seedling roots serves to mobilize and acquire *de novo* Fe from soil, a process relevant in the root epidermis. This subset is also referred to as “FIT-dependent” since its up-regulation requires the presence of a transcription factor called FIT (FER-LIKE FE DEFICIENCY-INDUCED TRANSCRIPTION FACTOR) (Schwarz & Bauer, 2020). A second subset is often

110 termed as "FIT-independent" since the expression of the genes in this cluster is particularly high when FIT
111 function is lost leading to the inability of acquiring *de novo* Fe hence induction of -Fe signals in the plant.
112 This subset of co-expressed genes is active in both, roots and shoots, and functions to mobilize and
113 allocate internal Fe from root to shoot or within the shoot and this subset is primarily expressed in the
114 root epidermis, root stele and in leaf vascular-associated tissues (Schwarz & Bauer, 2020). This co-
115 expression cluster encodes proteins that recycle Fe from vacuolar stores, transport Fe across tissues and
116 achieve long-distance phloem-based transport of Fe-nicotianamine chelates towards Fe sinks (Bastow et
117 al., 2018; Lanquar et al., 2005; Schuler et al., 2012), or control the management of metal ions (Haydon &
118 Cobbett, 2007). The concept of distinguishing coexpressed "FIT-dependent" and "FIT-independent" genes
119 has been applied to classify the hierarchy of Fe responses and decipher signaling and regulatory events
120 (Ivanov et al., 2012; Lichtblau et al., 2022; Muhammad et al., 2022; Schwarz & Bauer, 2020).

121 We hereby set out to investigate and correlate the -Fe responses of old and young rosette leaves
122 in spatial- and time-resolved manner across four reproductive stages. We recorded growth dynamics, Fe-
123 related gene expression changes and metal ion contents under +Fe and -Fe exposure. We hypothesized
124 that reproductive transition profoundly impacts Fe homeostasis, and we predicted an increase in -Fe
125 sensitivity in old and young leaves from early to late reproductive stages. However, this systematic study
126 uncovered unexpected dynamics on reproductive and stage-specific Fe homeostasis regulation under
127 changing Fe supply with distinct patterns in old and young leaves.

128

129 **Materials and Methods**

130 **Plant materials and growth conditions**

131 *Arabidopsis thaliana* ecotype Columbia (Col-0) seeds were surface-sterilized, stratified for 48
132 hours at 4°C in the dark and grown vertically on half-strength Hoagland agar plates (Lichtblau et al., 2022)
133 in a growth chamber (CLF Plant Climatics, Wertingen, Germany) at 16 h/8 h photoperiod with 100 µmol
134 m^{-2} s^{-1} light intensity, 22°C day/20°C night and 50 to 60 % relative humidity. 12-day-old seedlings were
135 transferred into a hydroponic setup as previously described by (Nguyen et al., 2016) using a quarter-
136 strength Hoagland hydroponic medium containing macronutrients (0.375 mM $MgSO_4$, 0.75 mM Ca $(NO_3)_2$,
137 0.25 mM KH_2PO_4, 0.625 mM KNO_3) and micronutrients (5 µM $MnSO_4$, 1 µM $ZnSO_4$, 0.75 µM $CuSO_4$, 0.0375
138 µM $(NH_4)_6Mo_7O_{24}$, 25 µM KCl, and 25 µM H_3BO_3). 25 µM FeNaEDTA was added to the nutrient medium as
139 sufficient Fe (+Fe). The medium was replaced every three days with freshly prepared hydroponic solution

140 aerated using air pumps. Plants were grown up to four reproductive stages as previously described in
141 (Boyes et al., 2001), hereby named the rosette stage (RS, early reproductive stage with <1cm inflorescence
142 stem and closed inflorescence bud, 24-day-old), bolting stage (BS, inflorescence stem 2-4cm with closed
143 inflorescence bud advanced inflorescence with beginning internode elongation, 32-day-old), flowering
144 stage (FS, main inflorescence stem >5cm with 3-5 open floral buds, 38-day-old) and mature silique stage
145 (MS, main inflorescence stem >8cm with 6-7 mature yellowing siliques, 46-day-old) (Figure 1A, Figure S1A,
146 B). At the selected stages, half of the plants were transferred to +Fe, and the other half was exposed to -
147 Fe. Fe treatments were started 3-4 hours after the growth chamber lights had switched on. -Fe hydroponic
148 solution was the same quarter-strength Hoagland medium described above, with no Fe supplementation
149 (0 µM FeNaEDTA). After 3 days of +Fe and –Fe treatment, roots, old leaves, young leaves and shoot apices
150 were excised. Leaves were pooled according to the scheme shown in Figure S1C for the different growth
151 stages. For leaf-by-leaf analysis, 3-week-old hydroponically grown plants were transferred at the RS to
152 +Fe or -Fe condition, and each day leaves were harvested from day 1 to day 7 for leaf area analysis.

153 **Determination of rosette and leaf size**

154 Plant rosette and leaf images were taken from the top using a Sony Alpha 6000 digital camera.
155 Images were imported into ImageJ version 1.8.0 (https://imagej.nih.gov/ij/) for further processing and
156 analysis. In brief, rosette images were converted to black and white and a color threshold set before
157 quantification of rosette area. The rosette area was calculated from the surface area covered by the
158 circumference of the longest leaves as shown in Figure 1B. Similarly, individual leaves were arranged in a
159 row from oldest to youngest leaf as illustrated in Figure S1C. Individual leaf areas were determined by the
160 area corresponding to that of the leaf blades.

161 **Scanning electron microscopy**

162 Hand-dissected shoot apices were fixed overnight in 1 % paraformaldehyde (PFA) solution then
163 dehydrated in a series of 30 %, 50 %, 70 % and 90 % ethanol, each for 20 min, and 100 % ethanol for 40
164 min. Samples were completely dehydrated to a critical point in a dryer (EMCPD 300, Leica) at 70 bar with
165 13°C /40°C cool-heat cycles for 3 hours. Samples were gold-coated under a high vacuum sputter (CCU-
166 010, Safematic) before imaging with an electron microscope (Supra 40VP, Zeiss). Images were analyzed in
167 ImageJ v 1.8.0.

168 **Gene expression analysis by reverse transcription (RT)-quantitative PCR (qPCR)**

169 All steps of RT-qPCR analysis were conducted according to (Ngigi & Bauer, 2023). Briefly, plant
170 materials were harvested and immediately deep-frozen in liquid nitrogen. Hand-dissected inflorescence
171 shoot apices, however, were first placed in RNAlater (Thermofisher Scientific) and then deep-frozen.
172 Samples were pulverized in a Precellys 24 tissue homogenizer (Peqlab, Germany). Total RNA extraction
173 from all plant samples was performed using a plant RNA kit (Qiagen, Germany). Approximately 1 µg of
174 RNA was treated with DNase I (Thermofisher Scientific) for removal of genomic DNA contamination
175 followed by first-strand cDNA synthesis using the Revert-aid reverse transcriptase kit (Thermofisher
176 Scientific). Real time qPCR was performed using 2x iTaq SYBR Green Supermix detection (Bio-Rad) on
177 C1000 Touch CFX384 (Bio-Rad). qPCR data were individually checked and validated by melt curve analysis.
178 Mean absolute normalized transcript abundances were calculated thanks to mass standard analysis and
179 referral to the expression of reference gene *EF1B-ALPHA2*. qPCR primer sequences are listed in
180 (Supplementary Table S1).

181 **Ionomics analysis**

182 Roots and leaves were collected. Residual Fe in the root apoplast was removed by washing the
183 roots in 20 mM Tris, 5 mM EDTA, pH 8 for 5 min before rinsing in deionized water. Old and young leaves
184 were washed in deionized water to remove Fe on the leaf surface. All samples were dried at 65°C for 3
185 days (or longer as needed) before grinding to a fine powder. Ground material was transferred into metal-
186 free 5 ml screw-cap tubes (Eppendorf, Germany, Cat. No. 0030122305) and 1 ml of 67 % nitric acid added.
187 Samples were digested by boiling until a clear liquid was obtained. Elemental analysis was performed
188 using inductively coupled plasma-mass spectroscopy (ICP-MS, Agilent 7700). A total of 5 plants were
189 pooled together for material collection per sample in three independent experiments. Elemental
190 concentrations were determined with the help of mass standards and normalized to sample dry weights.

191 **Statistical analysis and data visualization**

192 Data was analyzed by one-way analysis of variance (ANOVA) with Tukey's Honest Significant
193 Difference (HSD) test for multiple comparisons and Student's T test for pairwise comparisons. Bar graphs
194 and line charts show mean and standard deviation of 3-5 biological replicates. Means that were
195 statistically significantly different are indicated by different letters ($p < 0.05$). Correlation analysis of
196 normalized gene expression values and mineral content was done using Pearson's correlation with
197 significance p value < 0.05. Heatmaps were generated using mean absolute normalized gene expression
198 values. The data were processed using R (version 4.4.1). Gene names were assigned as row labels. Z-score

199 normalization was applied to each gene (row-wise) to account for variability in baseline expression. The
200 Z-scores were calculated using the scale () function in R, with the following formula:

201 $$Z = \frac{X - \mu}{\sigma}$$

202 where X is the expression for a specific sample, μ is the mean expression of the gene across all samples, σ
203 is the standard deviation of the gene expression. This row-wise Z-score normalization made it possible to
204 compare expression levels of each gene across tissues at both +Fe and -Fe, allowing positive Z-scores to
205 indicate above-average expression for high expression values and negative Z-scores to indicate below-
206 average expression for low expression values. The heatmaps were generated using the pheatmap package
207 in R.

208 **Results**

209 **The size of the leaf rosette increases during four reproductive phases**

210 To assess plant responses during the reproductive phase, Arabidopsis wild-type (Col-0) plants
211 were grown for up to seven weeks in sufficient Fe condition (+Fe) in a hydroponic system. Four meaningful
212 reproductive stages were selected for plant phenotyping (Figure 1A, Figure S1A, B). At the rosette stage
213 (RS, 24 days) plants did not yet have an emerged inflorescence stem, the rosette had approximately 11
214 emerged leaves, and plants had a closed inflorescence bud at the shoot apex (Figure 1A, Figure S1A-D). At
215 the bolting stage (BS, 32 days), the main inflorescence stem had emerged and was between 2 to 4 cm tall,
216 the rosette had around 11 examinable leaves which had grown bigger than at the RS, with closed floral
217 buds (BS, Figure 1A, Figure S1A-D). At the flowering stage (FS, 38 days), the main inflorescence stem had
218 elongated and was taller than 5 cm with 3-5 open flowers, the rosette had 13-17 amenable leaves (FS,
219 Figure 1A, Figure S1A-D). At the mature silique stage (MS, 46 days), more than three lateral inflorescence
220 branches had emerged, the main inflorescence stem was longer than 8 cm with 6-7 drying siliques, each
221 being longer than 1 cm, and the rosette had more than 20 amenable leaves (MS, Figure 1A, Figure S1A-
222 D). Rosette area is a commonly used parameter for growth evaluation of *A. thaliana* (Saini et al., 2022).
223 The rosette growth curve was rather steep (Figure 1B). Maximal rosette dimensions were reached at MS.
224 The fastest rosette size increase took place between RS and FS, particularly around BS, while it slowed
225 down before the RS and between FS and MS (Figure 1B). We suspected that Fe was needed for rosette
226 leaf growth to occur during the reproductive stages, particularly during the rapid size increase.

227

228 **Leaf sizes of young leaves were reduced in response to -Fe versus +Fe**

229 We tested whether leaf growth was linked with Fe availability. As according to a previous study,
230 we termed the fully grown leaves that had reached their final or nearly final size as "old leaves", while the
231 still developing leaves were termed "young leaves" (Schuler et al., 2012). It is reported that the sizes of
232 young leaves change upon micronutrient deficiency (Swartz et al., 2023). But whether rosette leaf growth
233 is still influenced at the reproductive growth stages is not yet known. We grew plants up to the four
234 selected reproductive stages and exposed them to +Fe and -Fe for 3 days. Individual leaves were dissected
235 (Figure S1C) and leaf areas measured, then grouped into old and young leaves taking into account the leaf
236 characteristics as described in (Swartz et al., 2023) (Figure S1C). There were no significant differences
237 between either old leaves or young leaves at +Fe and -Fe, respectively (Figure 1C-D). However, when
238 comparing the relative leaf area changes between -Fe versus +Fe, there were differences between old and
239 young leaves at BS, FS and MS (Figure 1E), which can be attributed to an age-dependent expansion during
240 early development phase. At the RS, old and young leaves had similar sizes when plants were exposed to
241 +Fe and -Fe treatments (Figure 1D), presumably because they were still small and not expanding as much
242 as during BS to MS.

243 To assess whether overall plant growth was also affected by -Fe treatment, we collected biomass
244 data. The root fresh weights had increased steadily from RS to MS. At the RS and BS, there were no
245 significant differences in root fresh weights after a +Fe and -Fe treatment, however, at FS and MS, there
246 was a drastic reduction of root fresh weight after the 3-day -Fe exposure compared with +Fe (Figure S1E).
247 Shoot biomass increased steadily from RS to MS. Particularly between FS and MS, shoot fresh weights had
248 drastically increased, but there was no difference following the 3-day +Fe and -Fe conditions (Figure S1F).
249 The shoot biomass increase was caused by the growing inflorescence stems, flowers and siliques, and
250 perhaps the growth differences could not be detected by total weight.

251 Taken together, our growth system is suited to detect Fe-dependent growth dynamics in the
252 rosette during the reproductive growth phases. In particular, the rapid increase of the sizes of young
253 leaves and the rosette visible at the BS is influenced by Fe supply and suppressed in response to -Fe. Since
254 the responses of rosette leaves during the reproductive phase are underexplored, we focused on rosette
255 leaf physiology in the continuation of this study.

256

257 **Leaf-by-leaf analysis during consecutive days displayed a rapid growth arrest of young leaves in**
258 **response to -Fe**

259 To better resolve the Fe-dependent influence on leaf growth, we selected the RS stage and
260 exposed plants to +Fe and -Fe. The rosette area and leaf sizes of the first up to ten amenable leaves were
261 determined on days 1, 2, 3, 5 and 7 (Figure 2). Between days 5 and 7, the rosette sizes of +Fe plants began
262 to increase rapidly, and at these timepoints, significant differences became apparent between +Fe and -
263 Fe-grown plants (Figure 2A-C). In the +Fe condition, rosette leaves displayed a green color throughout the
264 7-day period, while under -Fe conditions, the visual symptoms of leaf chlorosis became evident on day 2
265 and intensified as the experiment progressed (Figure 2A & B). Notably, -Fe leaf chlorosis was more
266 pronounced in the young leaves, e.g. L8 to L10, compared to old leaves, e.g. L3 to L5 (Figure 2B). The
267 young leaves e.g. leaf 8 were smaller at -Fe than +Fe from day 1 to day 7 (Figure 2D), similar to leaf 5 to
268 leaf 7 (Figure S2D-F). L3, an old leaf, did not show changes in the leaf areas on day 1 and day 5 to 7
269 irrespective of treatments, showing that they had reached their final size at the RS. However, L5 to L8
270 increased in size from day 1 until day 7, indicating they were continuously developing young leaves (Figure
271 2D and S2D-F). Interestingly, already after 1 day of -Fe treatment, the leaf areas were smaller in all these
272 four leaves compared to +Fe (L5 to L8) (Figure 2D and S2D-F). This shows that -Fe affected leaf growth
273 and expansion immediately within a day.

274 Taken together, these findings underscore the critical role of Fe for the growth of young leaves.
275 Young leaves were more susceptible to developing leaf chlorosis than old leaves. The differential
276 phenotypic responses observed between old and young leaves speak in favor of differential Fe
277 homeostasis physiology between old and young leaves. The very rapid growth response indicates that -Fe
278 sensing and signaling directly controls leaf growth.

279

280 **Expression of Fe-regulated genes points to Fe recycling taking place in old leaves at RS and BS**

281 To capture differential regulation patterns of leaves across the reproductive stages, we studied
282 the gene expression patterns of 23 Fe homeostasis genes by analyzing transcript amounts using reverse
283 transcription-qPCR, that corresponded to meaningful lists of genes from previously reported studies (Mai
284 et al., 2016; Schwarz & Bauer, 2020). We grew plants as above and collected old and young rosette leaves
285 of +Fe and -Fe plants across the four reproductive stages to investigate gene expression in space- and
286 time-resolved manner (old leaves were L3 to L5 from RS to FS, and L5 to L7 at MS, as L1 to L4 had senesced

287 at this stage; young leaves were L9 to L11 from RS to FS, and L14 to L17 at MS; Figure S1). Inflorescence
288 shoot apices were collected since they harbored the youngest leaves and leaf primordia. Roots were
289 harvested to estimate the Fe status of plants. The 23 analyzed genes were grouped into six categories or
290 clusters according to their previously described co-regulation and expression patterns, representing
291 different roles in Fe homeostasis (Figure 3A).

292 The gene expression data were remarkable in several ways. At first, we investigated gene
293 expression in the leaf and shoot apex samples. The FIT-independent RED -Fe cluster genes which serve
294 the recycling of Fe in the whole plant were overall expressed more under -Fe versus +Fe in both, the old
295 and young leaves, and the shoot apex samples (Figure 3B, C). In the leaf samples, this was particularly
296 evident at the early reproductive stages RS and BS where all 12 genes in the RED -Fe cluster were
297 expressed at higher level than at late reproductive stage, MS (Figure 3C). We see this observation as a hint
298 that the -Fe-induced RED cluster genes are not needed to be expressed strongly in the rosette leaves at
299 the late reproductive stages when siliques are developing. We suspect that at FS and MS the rosette leaves
300 become less susceptible to -Fe signals than at earlier stages. Surprisingly, gene expression of RED -Fe
301 cluster was remained induced in the inflorescence shoot apices at FS and MS, which provided a hint that
302 these genes regulated by Fe homeostasis in the reproductive shoot apical meristem. We noted another
303 interesting feature about the expression patterns of RED -Fe cluster genes, namely that their co-
304 expression was split in the +Fe samples. The four *BHLH* subgroup Ib genes (*BHLH038*, *BHLH039*, *BHLH100*
305 and *BHLH101)*, *NAS4*, *IMA1,* and *IMA3* genes were expressed at comparably low level at +Fe as compared
306 with *PYE*, *OPT3*, *FRO3*, *ZIF1* and *BTS*, which were more expressed at +Fe and even quite elevated in the
307 +Fe shoot apices. In sum, the -Fe regulation of RED -Fe cluster genes is most important in both old and
308 young leaves, in particular, at the BS and RS, as well as in the inflorescence shoot apices at all reproductive
309 stages. There is evidence that *PYE*, *OPT3*, *FRO3*, *ZIF1* and *BTS* are differently expressed from other RED -
310 Fe cluster genes, which can hint to different upstream regulation or functions.

311 Next interesting observation was that the expression of genes encoding the positive regulators of
312 RED -Fe cluster genes, namely *ILR3* and *BHLH104*, summarized as Upstream BHLH, and the negative
313 regulator, namely *BHLH11*, was consistent with that of the RED -Fe cluster genes *PYE*, *OPT3*, *FRO3*, *ZIF1*
314 and *BTS*. When these RED -Fe cluster genes were up-regulated specifically at BS under -Fe, it was also the
315 case for the positive regulators *ILR3* and *BHLH104*, while the negative regulator *BHLH11* was down-
316 regulated, especially in the old leaves. The upstream regulator genes were not Fe-regulated and were
317 expressed at BS to MS in old and young leaves, and in all the stages in inflorescence shoot apices (Figure

318 3B, C). For *ILR3* and *BHLH104*, this was expected, but for *BHLH11* it was unexpected, since it was reported
319 that BHLH11 is down-regulated by -Fe (Tanabe et al., 2019). With respect to a possible difference of
320 expression in old versus young leaves, we noted a tendency that at -Fe, expression was higher in old versus
321 young leaves in agreement with the expression of target RED -Fe cluster genes (Figure 3C).

322 Another remarkable point was, that High Fe marker *FER1* expression levels remained relatively
323 more highly expressed throughout the stages at +Fe in the old leaves compared to -Fe and young leaves
324 (Figure 3B). This was not the case for *FER4* expression. On the other hand, *FER1* and *FER4* showed similar
325 high expression in the inflorescence shoot apex samples across the stages at +Fe with slight
326 downregulation at -Fe (Figure 3B, C). Surprisingly, *NAS3* expression levels was consistently up in the young
327 leaves at all the four reproductive stages in both Fe conditions, but down in shoot apices (Figure 3B, C).
328 With respect to the question about differences in the leaf samples at -Fe, we noted tendencies of higher
329 expression of *FER1* and *FER4* in old versus young leaves, both of which were significant at MS whereas
330 *NAS3* was higher expressed in young versus old leaves across the four stages (Figure 3C). Thus, High Fe
331 marker gene expression did not distinguish the four reproductive stages, but it might be a marker for Fe-
332 regulated processes in the old versus young leaves and in the shoot apex. Perhaps *NAS3* plays a major role
333 in Fe remobilization and export.

334 Finally, *YSL3* was expressed at higher levels in leaves than in the shoot apex samples, and in some
335 cases, there appeared up-regulation at -Fe versus +Fe, such as at the BS in leaves (Figure 3B, C). *FRO7*, had
336 similar expression between +Fe and -Fe, but it was mostly expressed at higher levels in shoot apex samples
337 than in leaves, especially at MS (Figure 3B, C). Very interestingly, the expression of *YSL3* was up-regulated
338 in old versus young leaves at -Fe at all the four stages RS, BS, FS and MS. *FRO7* expression differences was
339 not noted between leaves and Fe supply (Figure 4B, C).

340 The root gene expression patterns were also very remarkable. As compared with rosette leaf and
341 shoot apex samples, the expression levels were surprisingly much lower for most genes analyzed above
342 (Figure S3). Although the FIT-dependent BLUE -Fe genes, previously known as root -Fe markers, were on
343 one side expressed at similar or higher levels in roots versus the shoot organs, but on the other side, an
344 exception was that the BLUE -Fe genes were quite strongly expressed at BS in the leaf samples, and at MS
345 in the shoot apex samples. Perhaps the root system is either no more very sensitive to -Fe or it also consists
346 of different zones that respond differently to -Fe.

347 Taken together, the leaf and shoot apex gene expression patterns were rather complex during
348 the reproductive stages. There were differences in expression between +Fe and -Fe, between the four
349 reproductive stages and between old and young leaves as well as inflorescence shoot apex. Two major
350 conclusions could be drawn. Fe recycling genes of the RED -Fe cluster were mostly expressed at the RS
351 and BS stages in old and young leaves at -Fe, while High Fe markers were rather uniformly expressed
352 throughout all stages at both +Fe and -Fe. Most genes that discriminated against old and young leaves
353 were expressed at higher levels in old versus young leaves, especially RED -Fe cluster genes *PYE*, *OPT3*,
354 *FRO3*, *ZIF1* and *BTS* and *YSL3* at -Fe, as well as *FER1* at +Fe and in the High Fe genes cluster. Only *NAS3*
355 was found to be consistently higher expressed in young than old leaves and shoot apices. These findings
356 indicate that different physiological states are associated with the organs at the different reproductive
357 stages.

358

359 **Mineral contents differ between old and young leaves at the early reproductive stages**

360 To test whether old and young leaves may be subject of different Fe and metal ion physiology, we
361 determined the elemental contents of Fe, Zn, Mn and Cu.

362 At first, we compared the elemental contents between +Fe and -Fe separately for old and young
363 leaves and roots (Figure 4). In old and young leaves, there was a clear trend that metal contents decreased
364 from RS to MS in the +Fe and -Fe conditions (Figure 4A, B, D, E, G, H, J, K). In old leaves, this was the case
365 for Zn and Mn at +Fe and -Fe (Figure 4D, G) and for Cu at -Fe (Figure 4J). In young leaves, it was the case
366 for all elements, however, in a Fe-dependent manner, such as for Fe and Mn at +Fe (Figure 4D, G), and for
367 Zn and Cu at both Fe supply conditions (Figure 4E, K). We then compared the elemental contents at each
368 stage between +Fe and -Fe in leaves. Surprisingly, there were not many differences in the old leaves when
369 we compared across the stages +Fe and -Fe conditions. In old leaves, there were no differences in Fe, Zn
370 and Mn contents between +Fe and -Fe treatments and across the growth stages (Figure 4A, D, G).
371 However, there was a difference in Cu contents, which had increased at RS in the old leaves (Figure 4J). In
372 young leaves, on the other hand, the Fe contents had clearly decreased between +Fe and -Fe from RS to
373 FS (Figure 4B). The Cu contents had again increased between +Fe and -Fe at the RS (Figure 4K). When
374 comparing between old and young leaves, the metal contents were either unchanged or lower in young
375 versus old leaves in the cases of Fe, Zn and Mn (Figure S4A-F). Only Cu amounts were higher in young than
376 in old leaves at BS under +Fe condition (Figure S4G). Hence, unlike young leaves, it seems that Fe was

377 likely not mobilized from old leaves during the reproductive stages at -Fe, and Fe was also not likely moved
378 from old to young leaves. This was different for Mn and Zn, which were likely mobilized in old and young
379 leaves as their contents decreased with progression of reproduction.

380 The root elemental contents supported that root uptake was dependent on Fe supply. As
381 expected, Fe contents were lower in roots at -Fe versus +Fe, even though this only occurred at BS and FS
382 (Figure 4C). Unexpectedly, the content of Zn was lower at RS and that of Mn was lower at MS when
383 comparing -Fe against +Fe (Figure 4F, I). Notably, the Cu content was up in -Fe versus +Fe roots at all
384 stages (Figure 4L), which presumably accounts for the elevated Cu contents in -Fe leaves at RS.

385 Hence, complex interactions in metal ion physiology were observed in old and young leaves at
386 +Fe and -Fe across the stages. -Fe affected Fe, Zn and Mn contents similarly, but had very different effects
387 on Cu contents both in leaves and roots. The highest metal ion contents were mostly observed at the early
388 reproductive stages, indicating a usage during progression to late reproductive development.

389 **Gene expression correlated with the mineral contents in leaves**

390 We investigated whether the gene expression levels correlated with mineral contents. Notably,
391 we observed positive correlations between Fe, Zn, Mn and Cu levels, in both old and young leaves at +Fe
392 and -Fe conditions. This confirmed an interaction in the mineral metal physiology in both leaf types under
393 changing Fe environments. Furthermore, we found meaningful correlations between mineral metal
394 contents with gene expression levels in old and young leaves (Figure 5).

395 In old leaves, Fe contents correlated positively with the three coexpressed RED -Fe genes *NAS4*,
396 *IMA1* and *IMA3* at +Fe, and with *BHLH038* at -Fe (Figure 5A). Negative correlations were found at -Fe
397 between Fe content and *BHLH11* and *FRO7* expression. Furthermore, in old leaves, Zn and Cu content
398 correlated positively with expression of RED -Fe genes *NAS4* and *FRO3* at +Fe, and *BHLH038* at -Fe. On the
399 other hand, *OPT3* negatively correlated with Mn and Cu levels under +Fe condition. Positive correlations
400 were seen between Zn, Mn and Cu amounts with *BHLH038* at -Fe, and negative correlations of these
401 minerals content with *FRO7* expression (Figure 5A).

402 In young leaves (Figure 5B), different correlations were seen, and most correlations were seen in
403 young leaves at -Fe. Fe contents correlated positively with *FRO3*, and negatively with *BTS* at +Fe. At -Fe,
404 the Fe amounts positively correlated with *FRO*3, and negatively with *BHLH039, ILR3 and BHLH104* gene
405 expression. There were positive correlations between Zn and Mn content and *FRO3* at +Fe (Figure 5B). At

406 similar Fe condition, negative correlations appeared between Zn and Cu with *BHLH038* and *FRO7*, while
407 Mn negatively correlated with *BHLH038, NAS4, OPT3* and *BTS* expression levels. When Fe was absent,
408 more positive correlations were observed between Zn content with *BHLH038/100, IMA1, PYE, FRO3 and*
409 *ZIF1*, but negatively with *FRO7*. Similar correlation patterns were observed with Cu amounts in the young
410 leaves at -Fe. Additionally, Cu amounts showed negative correlations with *FER4, NAS3 and FRO7*. Similar
411 to the old leaves, the contents of Fe, Zn, Mn and Cu in young leaves, positively correlated with each other
412 at both Fe conditions, except between Fe and Cu at -Fe.

413 In summary, the observed correlation patterns confirmed that the gene expression was indeed
414 linked with the mineral metal contents in the old and young leaves under +Fe and -Fe conditions. It was
415 also possible to distinguish old and young leaf Fe physiology by the correlations among gene expression
416 and metal contents. The mineral metal levels correlated with each other and may account for the
417 observed gene expression changes in the leaves.

418 **Discussion**

419 In this study, we investigated how reproductive transitions impact Fe and metal ion physiology in
420 rosette leaves when plants were exposed to +Fe and -Fe. Leaf growth especially between RS and FS was
421 markedly influenced by Fe availability, which indicates an interesting cross-connection with leaf signaling
422 events influencing leaf growth. Contrary to our idea that -Fe would cause important mobilization of Fe
423 from rosette leaves during late reproductive stages, our findings revealed unexpected stage-specific
424 dynamics in Fe and metal ion homeostasis. At the early reproductive stages, plants demonstrated a
425 stronger response to -Fe in the rosette leaves than at late reproductive stages, suggesting that rosette
426 leaves at late reproductive stages do not play important roles in metal ion homeostasis. Old and young
427 leaves reacted differently in terms of changes of metal contents and gene expression patterns in response
428 to +Fe and -Fe. The data indicate that old and young leaves can be sources and sinks for metal ions under
429 different Fe conditions.

430

431 **Growth of young leaves is rapidly inhibited at -Fe suggesting an intersection of -Fe and leaf growth**
432 **signaling**

433 Young leaf expansion was notably slowed and accompanied by leaf chlorosis following a 3-day -
434 Fe treatment, particularly during the rapid growth at the BS and FS. The inhibitory effect of -Fe on growth

435 and greening of young leaves was very rapid and became visible already after one day of -Fe. This fast Fe-
436 dependent leaf growth response demonstrates the high plasticity of young leaves in response to
437 environmental cues, in this case -Fe signals. Old leaves, instead, had already reached their final size so
438 that their growth response was unaffected. Leaf growth is the result of cell proliferation and cell expansion
439 (Li et al., 2024; Wu et al., 2009; Xu et al., 2016). We therefore suppose that the observed reduced leaf
440 sizes of young leaves could be a consequence of repression in growth and plasticity in these leaves upon
441 -Fe signals. Future studies will focus on dissecting the players at the intersection between regulation of
442 leaf growth and Fe homeostasis control.

443 It is known that leaf form and morphology change in response to environmental and
444 developmental cues and are especially common for the juvenile to adult leaf transition, which is caused
445 by a process referred to as leaf heteroblastic reprogramming (Bäurle & Dean; Costa et al., 2012; Tsukaya,
446 2005; Tsukaya et al., 2000). In *Arabidopsis thaliana,* SQUAMOSA PROMOTER BINDING PROTEIN-LIKE 9
447 (SPL9) targeted by miR156 regulates the juvenile-to-adult transition which influences leaf morphology
448 (Wu et al., 2009; Xu et al., 2016). Mechanisms for leaf development transition and Fe homeostasis have
449 been proposed for the miR156-SPL9 module, whereby SPL9 transcriptionally could regulate Fe deficiency
450 markers *FIT* and *PYE* by direct promoter binding (Wang 2015), a model requiring further investigation.
451 Furthermore, in rice, *OsSPL9*, an ortholog of *SPL9* in *Arabidopsis*, has been proposed to be involved in Cu
452 deficiency response whereby a knockout *spl9* mutant was sensitive to Cu deficiency with reduced
453 accumulation of Cu in the old versus young leaves (Wang et al., 2024). These studies confirm that indeed
454 SPL9, among other leaf growth regulators, may influence mineral uptake responses to synchronize
455 development with nutrient availability. Thus, it is possible that in our system, -Fe signals influenced
456 expression levels of leaf growth regulators. Future studies may investigate Fe responses using mutants
457 defective in leaf cell proliferation and elongation, for example, using plants with *SPL9* mutations which
458 were shown to have defects in leaf cell expansion during the juvenile-to-adult transitioning (Li et al., 2024).

459 On the other hand, retrograde chloroplast signaling can also affect cell expansion and leaf
460 greening (Andriankaja et al., 2012). Inferring from this, it is also a possibility that in our system, -Fe signals
461 acted to inhibit leaf cell expansion and greening by blocking retrograde signaling. In such a scenario, -Fe
462 signaling to the chloroplasts repress signals towards the nucleus and inhibit expression of nuclear-
463 encoded leaf development- and photosynthesis-related genes. Previous studies have addressed
464 retrograde signaling upon -Fe (Balparda et al., 2020, 2021). Alternatively, retrograde chloroplast signals
465 may be activated under -Fe but then block the reprogramming in the nucleus thus influencing downstream

466 transcription of photosynthesis and growth regulators (Nam et al., 2021). -Fe-induced transcription
467 factors including the class 1b bHLH might be able to interact with the transcriptional regulation apparatus
468 for leaf cell differentiation, thus regulating leaf cell proliferation and expansion as demonstrated before
469 (Andriankaja et al., 2014). TCP transcription factors, that positively control leaf expansion can bind with -
470 Fe-induced bHLH subgroup Ib proteins and transcriptionally repress their expression (Andriankaja et al.,
471 2012). However, in these studies, bHLH subgroup Ib transcription factors seemed to be induced during
472 the transition phase from cell proliferation to cell expansion at +Fe in early leaf growth phases. This
473 appears contradictory to our -Fe data where these genes were induced in old leaves as well. Nevertheless,
474 it needs to be taken into account that these previous studies investigated seedling stages while we
475 focused on later reproductive stages which may account for such differences.

476

477 **Distinct Fe physiology in early and late reproductive stages and in old and young leaves**

478 Rosette leaves display more distinctive Fe physiology responses at +Fe at the RS and BS than at
479 late reproductive stages. The gene expression patterns and metal contents indicate that at the early
480 reproductive stages, metal ion physiology is more active than at late reproductive stages. For example, Fe
481 recycling genes (RED -Fe genes) *NAS4*, *OPT3*, and *FRO3* which play a key role in Fe redistribution between
482 source and sinks (Khan et al., 2018; Kumar et al., 2017; Nguyen et al., 2022; Schuler et al., 2012; Stacey et
483 al., 2008), were upregulated in both old and young leaves at RS and BS. This showed that Fe mobilization
484 responses in old and young leaves were highly induced during these stages. Studies have demonstrated
485 that Fe fluxes increase between the rosette and the inflorescence organs including stems, fruits and seeds
486 after onset of flowering (Mendoza-Cózatl et al., 2014; Pottier et al., 2019; Waters & Grusak, 2008; Zhai et
487 al., 2014). On the other hand, High Fe genes like *FER1* and *NAS3* were expressed similarly throughout the
488 four stages in old and young leaves respectively, while a marker for internal Fe mobilization from the
489 chloroplast, *FRO7*, was predominantly expressed at the FS and MS stages in both leaves. This can indicate
490 that Fe recycling from subcellular storage involving the RED -Fe genes is more important at the early
491 reproductive stages. At these stages, old leaves can be sources of Fe and other metal ions for supply to
492 sink organs including developing leaves and inflorescence stems. At the later reproductive stages, Fe
493 remobilization from plastids involving genes like *FRO7* may be switched on. Fe is mobilized from plastids
494 at the onset of leaf senescence and may prepare for Fe allocation towards seed filling (Himelblau &
495 Amasino, 2001). Senescence takes place in the older leaves and can be triggered by plant age and
496 environmental cues in order to enhance plant resilience to stress conditions and efficiently use nutrients

497 (Buchanan-Wollaston, 1997; Lemaître et al., 2008; Nooden et al., 1996; Sperotto et al., 2012; Waters et
498 al., 2009). Leaf senescence can lower the sensitivity to external -Fe as plants instead mobilize intracellular
499 Fe stores in the vegetative organs instead of *de novo* uptake by the roots (Pottier et al., 2019). Additionally,
500 resulting oxidative stress responses due to internal Fe release may induce expression of High Fe gene
501 cluster in leaves consequently dampening Fe uptake responses in roots (Le et al., 2016). Rosette leaves
502 are the targets of xylem mineral transport. There was a drastic decrease of Mn and Zn in old and young
503 leaves and a decrease of Fe and Cu contents in young leaves at +Fe from RS towards MS, indicating that
504 at late reproductive stages metals may have been exported from the rosette leaves to replenish sinks
505 forming in the inflorescence such as fruits and seeds. It is likely that at the late reproductive stages the
506 xylem stream is oriented towards the inflorescence stem directly rather than the rosette leaves so that
507 cauline leaves and inflorescence stems account primarily for allocation of Fe, taken up de novo and
508 transported from roots to seeds (Pottier et al., 2019; Schuler et al., 2012; Waters & Grusak, 2008). The
509 enhanced -Fe responsiveness in the shoot apex samples even at FS and MS speaks in favor of this. In future
510 studies it can be investigated whether new Fe storage tissues arise during reproductive growth in addition
511 to the rosette leaves, e.g. in the secondary phloem tissues coupled with secondary growth in the
512 Arabidopsis hypocotyl during flowering (Lehmann & Hardtke, 2016; Wunderling et al., 2018).

513 Notably, particular observations were highly interesting and striking. One remarkable observation
514 was that the differential expression of RED -Fe genes in the old leaves at -Fe indicated a
515 subfunctionalization among RED -Fe gene functions. The expression regulation of subgroup Ib *BHLH*, *IMA*
516 and *NAS4* genes could be distinguished from that of *PYE*, *OPT3*, *FRO3*, *ZIF1* and *BTS*. PYE negatively
517 regulates certain RED -Fe genes, including *bHLH1B* genes, *FRO3*, *ZIF1* and *NAS4* in seedlings (Haydon et
518 al., 2012; Long et al., 2010; Pu & Liang, 2023; Schuler, 2011). Possibly, individual regulator proteins such
519 as PYE, BTS or upstream transcription factors have individual functions in controlling positively or
520 negatively different subsets of Fe mobilization and Fe storage genes in different tissues (Akmakjian et al.,
521 2021; Muhammad et al., 2022; Rodríguez-Celma et al., 2019; Zhang et al., 2015) and at different
522 developmental stages. Future studies can focus on investigating the roles of regulatory genes not only
523 during early vegetative seedling stages but also during reproductive stages.

524 Another observation was interesting, namely the increase of Cu contents in old and young leaves
525 at the RS following the -Fe treatment. This Cu increase was certainly linked with the very high Cu uptake
526 into roots at -Fe. It indicates that despite their growth inhibition, the young leaves accumulated high Cu
527 amounts at this stage. There are evidences for Fe and Cu crosstalk whereby Cu amounts in roots and

528 shoots are increased at -Fe, and vice versa (Bernal et al., 2012; Carrió-Seguí et al., 2019; Chia et al., 2023;
529 Kastoori Ramamurthy et al., 2018; Rai et al., 2021; Waters & Armbrust, 2013). One of the genes encoding
530 a transporter for Cu uptake is *COPT2* which is a FIT target and upregulated under -Fe (Colangelo &
531 Guerinot, 2004). FIT protein also interferes with Cu regulators (Cai et al., 2021; Perea-García et al., 2020)
532 . This observation raises the question whether the gene expression changes and leaf growth suppression
533 can truly be attributed to -Fe or whether it could be a secondary consequence of elevated Cu.
534 Nicotianamine is a metal chelator for Cu and Fe, and Cu homeostasis is equally important for reproduction
535 than Fe (Sheng et al., 2021). -Fe was also reported to cause Zn and Mn accumulation in seedlings due to
536 the elevated IRT1 activity leading to the uptake of other bivalent metals including Fe, Zn and Mn (Cointry
537 & Vert, 2019; Dubeaux et al., 2018). Since we did not see this effect of Zn and Mn accumulation in -Fe in
538 roots and rosette leaves at the reproductive stage, except for elevated Mn at MS in roots, it is possible
539 that IRT1 function has a different relevance during reproduction or that mechanisms are in place to
540 repress metal uptake and transport to rosette leaves targeting Mn and Zn, thus preventing over
541 accumulation.

542

543 **Future perspectives**

544 The results of this study indicate a clear and significant negative impact of Fe deficiency on rosette
545 and young leaf growth dynamics, as well as the mineral partitioning in *Arabidopsis thaliana* during the
546 reproductive stages. The findings underscore the crucial role of Fe in plant growth at reproductive stages
547 and complex interactions and signaling between the various plant parts. This underlines that more
548 attention should be paid to the roles of Fe homeostasis genes in the reproductive stages. Further analysis
549 is thus required to elucidate the molecular mechanisms acting during reproduction. Our study was limited
550 by two aspects. On one side, only wild type Col-0 plants were investigated. Future studies shall focus on
551 natural variation and mutants of individual genes to undermine their roles in reproduction. On the other
552 side, conclusions are based on gene expression and metal contents, excluding the physiological roles of
553 the encoded transport proteins and enzymes. These components are subject of post-translational and
554 protein control, and clearly mutants affected in such regulatory mechanisms can reveal the contributions
555 during reproductive stages.

556 The question arises whether old leaves can be considered as Fe sources and whether young leaves
557 are Fe sinks at +Fe (Hantzis et al., 2018; Nguyen et al., 2022; Swartz et al., 2023). The here-established

558 growth system can be utilized to test such questions by performing Fe supply experiments in combination
559 with mutants that cannot steer Fe physiology properly at the reproductive stage. In the future, it will be
560 interesting to investigate the molecular mechanisms regulating potentially systemic Fe signals from
561 source to sinks in the rosette, and link gene expression with leaf growth signaling under +Fe and -Fe, e.g.
562 by utilizing SPL9 mutants or investigating the role of retrograde signaling pathway in leaf-to-leaf
563 communication.

564 Finally, analyzing gene expressions at the reproductive phase is challenging, since variations in
565 gene expression are relatively high and the whole plant physiology far more complex than in young
566 seedlings. Whole transcriptome studies will offer better insight into the general physiology of old and
567 young leaves and more complete investigation of Fe homeostasis genes in the future.

568 **Acknowledgements**

569 The authors thank Sabine Metzger, University of Cologne, for technical support in the ICP-MS
570 measurements. We acknowledge Rainer Franzen, Max Planck Institute for Plant Breeding Research
571 Cologne, for help with SEM imaging of inflorescence shoot apices. We thank Elke Wieneke, Monique
572 Eutebach and Florian Pollmeyer, all from Heinrich Heine University Düsseldorf, for excellent technical
573 support. We thank Hans-Jörg Mai, Heinrich Heine University Düsseldorf, for his helpful suggestions
574 regarding data visualization and manuscript figures. This work received funding by Deutsche
575 Forschungsgemeinschaft (DFG, German Research Foundation) under Germany´s Excellence Strategy –
576 EXC-2048/1 – project ID 390686111.

577

578 **Author contributions**

579 Conceptualization (M.N., M.K., P.B.), Methodology (M.N., M.K., R.R.), Investigation (M.N., R.R.),
580 Data Analysis (M.N., M.K., R.R., S.G.), Writing of Original Draft (M.N., M.K., P.B), Review & Editing (all
581 authors), Supervision (M.K., P.B.), and Funding Acquisition (P.B.).

582

583 **Figure 1. Growth dynamics during progression of the *Arabidopsis* life cycle.** (A) Overview of experimental
584 setup and reproductive growth stages selected for analysis of *Arabidopsis thaliana*. Seedlings were
585 germinated on Hoagland agar plates before transplanting to standard hydroponic media with 25 µM Fe

586 (+Fe) for growth to the four selected stages under long-day conditions; rosette stage (RS), bolting stage
587 (BS), flowering stage (FS) and mature silique stage (MS) before further analysis, scale bar = 1cm. Further
588 details on the reproductive growth stages in Figure S1A, B. (B) Rosette area increase of plants continuously
589 grown on media with +Fe until the mature stage. Rosette area included all leaves forming around the
590 canopy plus their petioles (*n* = 2-8). (C-D) Absolute leaf areas of old and young leaves at +Fe and –Fe,
591 respectively. Plants were transferred to +Fe and –Fe conditions for 3 days at the indicated growth stages.
592 Old and young leaves harvested for analysis are described in Figure S1C. (E) Relative changes in leaf area
593 sizes of old and young leaves under –Fe compared to +Fe conditions at the stages RS to MS. Data in (C-D)
594 represent average values of biological replicates (*n*=5). Error bars show ± SD. Statistical analysis was done
595 by Student's t-test ($p < 0.05$).

596

597 **Figure 2. Leaf-by-leaf analysis of *Arabidopsis thaliana* at the rosette stage (RS).** (A) At the RS, plants were
598 transferred to respective Fe sufficient (+Fe) or deficient (-Fe) Hoagland media solutions and growth
599 recorded from day 0 till day 7. (B) Leaf images of leaf 1 (L1) to 10 (L10) at the two Fe conditions, as
600 indicated. (C) Cumulative rosette area as recorded from (A). Data represent means of biological replicates
601 (*n*=3). Error bars represent ± SD. Statistical analysis was done using one-way ANOVA and Tukey's HSD test.
602 Means followed by the same letter are not significantly different ($p < 0.05$). (D) Radial charts showing the
603 leaf sizes of leaf 3 and 8 after exposure to either +Fe (control) or –Fe conditions from day 1 to day 7. Radial
604 charts were plotted in R Studio using "fsmb" package. Plants were grown for 3 weeks before culturing in
605 either +Fe or -Fe conditions.

606

607 **Figure 3. Gene expression analysis of selected Fe homeostasis genes.** (A) Schematic illustration showing
608 connections and functions of Fe homeostasis genes used in gene expression analysis. Represented is the
609 Fe-regulated transcriptional cascade and multiple layers of co-expressed genes involved in plant Fe
610 homeostasis. Exemplary references: [1](Kobayashi et al., 2021), [2](Zhang et al., 2015), [3](Lichtblau et al.,
611 2022), [4](Li et al., 2016), [5](Tanabe et al., 2018), [6](Trofimov et al., 2019), [7](Long et al., 2010), [8](Tissot et al.,
612 2019), [9](Chu et al., 2010), [10](Mukherjee et al., 2006), [11](Schuler et al., 2012). (B-C) Heatmaps showing the
613 absolute expression profiles of 20 selected Fe homeostasis genes in old leaves, young leaves, and

614 inflorescence shoot apices after exposure to +Fe and –Fe for 3 days. Plants were grown to the various
615 stages, as indicated, before transfer to either Fe solutions. The growth stages RS, BS, FS and MS
616 correspond to rosette stage, bolting stage, flowering stage and mature stage, respectively. Heatmaps
617 were generated in R studio version 4.4.1 using calculated z-scores of normalized gene expression values
618 of each gene across tissues for both +Fe and –Fe. Category annotations are displayed on the left side of
619 the heatmap, with tissue-type annotations displayed on the top. The colour scale ranges from -2 to 2 to
620 represent the variation in gene expression. Red colours represent gene up-regulation, and blue colours
621 represent gene down-regulation, $p < 0.05$ ($n = 3$).

622

623 **Figure 4. Ionomic analysis of leaves and roots.** Fe (A-C), Zn (D-F), Mn (G-I), and Cu (J-L) content per dry
624 weight (D.W.) in old leaves, young leaves and roots of plants grown at 25 µM Fe (+Fe) or 0 µM Fe (–Fe)
625 conditions and at the four growth stages; RS, BS, FS and MS. Plants were exposed to 3 days of +Fe or –Fe
626 before sample collection. Data represents mean of three biological replicates (*n* = 3). Error bars represent
627 ± SD. Letters on top of each bar show level of significance according to Tukey's HSD test, $p < 0.05$.

628

629 **Figure 5. Correlation analysis between gene expression changes and ionomic contents.** Correlations
630 were performed with data from old leaves (A), and young leaves (B) at +Fe (right side) and -Fe (left side)
631 conditions. Analysis was done using averages of normalized gene expression values and mineral
632 concentrations of Fe (Fe Conc.), Zn (Zn Conc.), Mn (Mn Conc.) and Cu (Cu Conc.) across all four stages RS,
633 BS, FS, and MS. Color scale represents Pearson's correlation coefficients normalized in the range between
634 -1 to 1, whereby -1 is negative correlations and 1 is positive correlations calculated between genes and
635 mineral content pair. Significant correlations at $p < 0.05$ are displayed in the diagram. (C) Table showing
636 summary of the number of correlations between either mineral-to-mineral content, mineral content to
637 gene expression level and correlation of gene gene-to-gene expression level. Numbers show total number
638 of positive and negative correlations at both +Fe and –Fe conditions.

639

640 **Figure S1.** Materials collected from *Arabidopsis thaliana* plants. (A) Top view of plants with their rosette
641 leaves at each stage, scale bar = 1cm. (B) Descriptions of the growth stages distinguishing phenotypes as

642 described by (Boyes et al., 2001). (C) Old (left) and young (right) leaves collected from plants at the
643 respective stages under +Fe (control) and –Fe after 3 days, scale bar = 1cm. (D) Scanning electron
644 microscopy images of inflorescence shoot apical meristems dissected from the main stems of plants at
645 the rosette to mature stages, scale bar = 100 µm. (E-F) Root and shoot fresh weights of plants grown to
646 RS, BS, FS, and MS and transferred to hydroponic media with +Fe or -Fe for 3 days. Data represents mean
647 of three biological replicates (*n* = 3). Error bars represent ± SD.

648

649 **Figure S2.** Radial charts showing the leaf sizes at +Fe and -Fe**.** (A-F) Individual leaf sizes of plants (L1, L2,
650 L4, L5, L6 and L7) at RS after exposure to either Fe sufficient (+Fe) or deficient (-Fe) conditions from day 1
651 to day 7, as indicated. Data represents the average of biological replicates (*n*=3). Radial charts were
652 plotted in R Studio using "fsmb" package.

653

654 **Figure S3. Gene expression analysis of selected Fe homeostasis genes in leaves, shoot apices and roots.**
655 (A-B) Heatmaps showing the absolute expression profile of Fe-response markers in roots, old leaves,
656 young leaves, and inflorescence shoot apex +Fe and –Fe respectively, for 3 days at RS, BS, FS and MS.
657 Heatmaps were generated in R studio version 4.4.1 using calculated z-scores of normalized gene
658 expression values of each gene across tissues for both +Fe and –Fe. Category annotations are displayed
659 on the left side of the heatmap, with tissue-type annotations displayed on the top. The colour scale ranges
660 from -2 to 2 to represent the variation in gene expression. Red colours represent gene up-regulation, and
661 blue colours represent gene down-regulation, $p < 0.05$ (n = 3).

662

663 **Figure S4. Comparison of mineral contents in old (OL) and young (YL) leaves at +Fe and –Fe growth**
664 **conditions.** Fe (A-B), Zn (C-D), Mn (E-F), and Cu (G-H) contents per dry weight (D.W.) in old leaves and
665 young leaves at +Fe or –Fe growth conditions at the growth stages; RS, BS, FS and MS. Plants were exposed
666 to 3 days of +Fe or –Fe before sample collection. Data represents mean of three biological replicates (*n* =
667 3). Error bars represent ± SD. Letters on top of each bar show level of significance according to Tukey's
668 HSD test, $p < 0.05$.

669

670 **Table S1.** List of primers used for gene expression analysis by reverse transcription-qPCR. Primers were
671 designed as previously described in (Ngigi & Bauer, 2023). Mass standard (STD) and real time qPCR (RT)
672 primers annealed to the indicated genes. Mass standard PCR products were used for absolute
673 quantification of transcript abundances of the respective genes.

674

675 **References**

676 Akmakjian, G. Z., Riaz, N., & Guerinot, M. L. (2021). *Photoprotection during iron deficiency is*
677 *mediated by the bHLH transcription factors PYE and ILR3*. https://doi.org/10.1073/pnas.2024918118/-
678 /DCSupplemental

679 Andriankaja, M., Dhondt, S., De Bodt, S., Vanhaeren, H., Coppens, F., De Milde, L., Mühlenbock,
680 P., Skirycz, A., Gonzalez, N., Beemster, G. T. S., & Inzé, D. (2012). Exit from Proliferation during Leaf
681 Development in *Arabidopsis thaliana*: A Not-So-Gradual Process. *Developmental Cell*, *22*(1), 64–78.
682 https://doi.org/10.1016/j.devcel.2011.11.011

683 Andriankaja, M. E., Danisman, S., Mignolet-Spruyt, L. F., Claeys, H., Kochanke, I., Vermeersch,
684 M., De Milde, L., De Bodt, S., Storme, V., Skirycz, A., Maurer, F., Bauer, P., Mühlenbock, P., Van
685 Breusegem, F., Angenent, G. C., Immink, R. G. H., & Inzé, D. (2014). Transcriptional coordination
686 between leaf cell differentiation and chloroplast development established by TCP20 and the subgroup Ib
687 bHLH transcription factors. *Plant Molecular Biology*, *85*(3), 233–245. https://doi.org/10.1007/s11103-
688 014-0180-2

689 Balparda, M., Armas, A. M., Estavillo, G. M., Roschzttardtz, H., Pagani, M. A., & Gomez-Casati, D.
690 F. (2020). The PAP/SAL1 retrograde signaling pathway is involved in iron homeostasis. *Plant Molecular*
691 *Biology*, *102*(3), Article 3. https://doi.org/10.1007/s11103-019-00950-7

692 Balparda, M., Armas, A. M., Gomez-Casati, D. F., & Pagani, M. A. (2021). PAP/SAL1 retrograde
693 signaling pathway modulates iron deficiency response in alkaline soils. *Plant Science*, *304*, 110808.
694 https://doi.org/10.1016/j.plantsci.2020.110808

695 Bastow, E. L., Garcia de la Torre, V. S., Maclean, A. E., Green, R. T., Merlot, S., Thomine, S., &
696 Balk, J. (2018). Vacuolar iron stores gated by NRAMP3 and NRAMP4 are the primary source of iron in
697 germinating seeds. *Plant Physiology*, *177*(3), 1267–1276. https://doi.org/10.1104/pp.18.00478

698 Bäurle, I., & Dean, C. (n.d.). *The Timing of Developmental Transitions in Plants*. Retrieved
699 November 3, 2024, from https://www.cell.com/cell/abstract/S0092-8674(06)00571-X

700 Bernal, M., Casero, D., Singh, V., Wilson, G. T., Grande, A., Yang, H., Dodani, S. C., Pellegrini, M.,
701 Huijser, P., Connolly, E. L., Merchant, S. S., & Krämer, U. (2012). Transcriptome Sequencing Identifies

SPL7-Regulated Copper Acquisition Genes FRO4/FRO5 and the Copper Dependence of Iron Homeostasis in Arabidopsis. *The Plant Cell*, *24*(2), 738–761. https://doi.org/10.1105/tpc.111.090431

Boyes, D. C., Zayed, A. M., Ascenzi, R., Mccaskill, A. J., Hoffman, N. E., Davis, K. R., & Görlach, J. (2001). Growth Stage-Based Phenotypic Analysis of Arabidopsis: A Model for High Throughput Functional Genomics in Plants. *The Plant Cell*, *13*, 1499–1510.

Briat, J. F., Curie, C., & Gaymard, F. (2007). Iron utilization and metabolism in plants. *Current Opinion in Plant Biology*, *10*(3), 276–282. https://doi.org/10.1016/J.PBI.2007.04.003

Buchanan-Wollaston, V. (1997). The molecular biology of leaf senescence. *Journal of Experimental Botany*, *48*(2), 181–199. https://doi.org/10.1093/jxb/48.2.181

Cai, Y., Li, Y., & Liang, G. (2021). FIT and bHLH Ib transcription factors modulate iron and copper crosstalk in Arabidopsis. *Plant, Cell & Environment*, *44*(5), 1679–1691. https://doi.org/10.1111/pce.14000

Carrió-Seguí, À., Romero, P., Curie, C., Mari, S., & Peñarrubia, L. (2019). Copper transporter COPT5 participates in the crosstalk between vacuolar copper and iron pools mobilisation. *Scientific Reports*, *9*(1), Article 1. https://doi.org/10.1038/s41598-018-38005-4

Chia, J.-C., Yan, J., Ishka, M. R., Faulkner, M. M., Simons, E., Huang, R., Smieska, L., Woll, A., Tappero, R., Kiss, A., Jiao, C., Fei, Z., Kochian, L. V., Walker, E., Piñeros, M., & Vatamaniuk, O. K. (2023). Loss of OPT3 function decreases phloem copper levels and impairs crosstalk between copper and iron homeostasis and shoot-to-root signaling in *Arabidopsis thaliana*. *The Plant Cell*, koad053. https://doi.org/10.1093/plcell/koad053

Chu, H.-H., Chiecko, J., Punshon, T., Lanzirotti, A., Lahner, B., Salt, D. E., & Walker, E. L. (2010). Successful Reproduction Requires the Function of Arabidopsis YELLOW STRIPE-LIKE1 and YELLOW STRIPE-LIKE3 Metal-Nicotianamine Transporters in Both Vegetative and Reproductive Structures 1[W][OA]. *Plant Physiology Ò*, *154*, 197–210. https://doi.org/10.1104/pp.110.159103

Cointry, V., & Vert, G. (2019). The bifunctional transporter-receptor IRT1 at the heart of metal sensing and signalling. *New Phytologist*, *223*(3), 1173–1178. https://doi.org/10.1111/nph.15826

Colangelo, E. P., & Guerinot, M. L. (2004). The Essential Basic Helix-Loop-Helix Protein FIT1 Is Required for the Iron Deficiency Response. *The Plant Cell*, *16*(12), 3400–3412. https://doi.org/10.1105/tpc.104.024315

Costa, M. M. R., Yang, S., Critchley, J., Feng, X., Wilson, Y., Langlade, N., Copsey, L., & Hudson, A. (2012). The genetic basis for natural variation in heteroblasty in Antirrhinum. *New Phytologist*, *196*(4), 1251–1259. https://doi.org/10.1111/j.1469-8137.2012.04347.x

Dubeaux, G., Neveu, J., Zelazny, E., & Vert, G. (2018). Metal Sensing by the IRT1 Transporter-Receptor Orchestrates Its Own Degradation and Plant Metal Nutrition. *Molecular Cell*, *69*(6), 953-964.e5. https://doi.org/10.1016/j.molcel.2018.02.009

Hantzis, L. J., Kroh, G. E., Jahn, C. E., Cantrell, M., Peers, G., Pilon, M., & Raveta, K. (2018). A Program for Iron Economy during Deficiency Targets Specific Fe Proteins. *Plant Physiology*, *176*(1), 596–610. https://doi.org/10.1104/PP.17.01497

Haydon, M. J., & Cobbett, C. S. (2007). A Novel Major Facilitator Superfamily Protein at the Tonoplast Influences Zinc Tolerance and Accumulation in Arabidopsis. *Plant Physiology*, *143*(4), 1705–1719. https://doi.org/10.1104/pp.106.092015

Haydon, M. J., Kawachi, M., Wirtz, M., Hillmer, S., Diger Hell, R., & A novel major facilitator superfamily protein at the tonoplast influences zinc toleranceKrä Mer, U. (2012). *Vacuolar nicotianamine has critical and distinct roles under iron deficiency and for zinc sequestration in Arabidopsis*. https://doi.org/10.1105/tpc.111.095042

Himelblau, E., & Amasino, R. M. (2001). Nutrients mobilized from leaves of Arabidopsis thaliana during leaf senescence. *Journal of Plant Physiology*, *158*(10), 1317–1323. https://doi.org/10.1078/0176-1617-00608

Ivanov, R., Brumbarova, T., & Bauer, P. (2012a). Fitting into the Harsh Reality: Regulation of Iron-deficiency Responses in Dicotyledonous Plants. *Molecular Plant*, *5*(1), 27–42. https://doi.org/10.1093/mp/ssr065

Ivanov, R., Brumbarova, T., & Bauer, P. (2012b). Fitting into the harsh reality: Regulation of iron-deficiency responses in dicotyledonous plants. *Molecular Plant*, *5*(1), 27–42. https://doi.org/10.1093/mp/ssr065

Jeong, J., & Guerinot, M. L. (2009). Homing in on iron homeostasis in plants. *Trends in Plant Science*, *14*(5), 280–285. https://doi.org/10.1016/j.tplants.2009.02.006

Kastoori Ramamurthy, R., Xiang, Q., Hsieh, E.-J., Liu, K., Zhang, C., & Waters, B. M. (2018). New aspects of iron–copper crosstalk uncovered by transcriptomic characterization of Col-0 and the copper uptake mutant spl7 in Arabidopsis thaliana†. *Metallomics*, *10*(12), 1824–1840. https://doi.org/10.1039/c8mt00287h

Khan, M. A., Castro-Guerrero, N. A., McInturf, S. A., Nguyen, N. T., Dame, A. N., Wang, J., Bindbeutel, R. K., Joshi, T., Jurisson, S. S., Nusinow, D. A., & Mendoza-Cozatl, D. G. (2018). Changes in iron availability in Arabidopsis are rapidly sensed in the leaf vasculature and impaired sensing leads to opposite transcriptional programs in leaves and roots. *Plant, Cell & Environment*, *41*(10), 2263–2276. https://doi.org/10.1111/PCE.13192

Kobayashi, T., Nagano, A. J., & Nishizawa, N. K. (2021). Iron deficiency-inducible peptide-coding genes OsIMA1 and OsIMA2 positively regulate a major pathway of iron uptake and translocation in rice. *Journal of Experimental Botany*, *72*(6), 2196–2211. https://doi.org/10.1093/jxb/eraa546

Kumar, R. K., Chu, H. H., Abundis, C., Vasques, K., Rodriguez, D. C., Chia, J. C., Huang, R., Vatamaniuk, O. K., & Walker, E. L. (2017). Iron-Nicotianamine Transporters Are Required for Proper Long Distance Iron Signaling. *Plant Physiology*, *175*(3), 1254–1268. https://doi.org/10.1104/PP.17.00821

Lanquar, V., Lelièvre, F., Bolte, S., Hamès, C., Alcon, C., Neumann, D., Vansuyt, G., Curie, C., Schröder, A., Krämer, U., Barbier-Brygoo, H., & Thomine, S. (2005). Mobilization of vacuolar iron by

775 AtNRAMP3 and AtNRAMP4 is essential for seed germination on low iron. *The EMBO Journal*, *24*(23),
776 4041. https://doi.org/10.1038/SJ.EMBOJ.7600864

777 Le, C. T. T., Brumbarova, T., Ivanov, R., Stoof, C., Weber, E., Mohrbacher, J., Fink-Straube, C., &
778 Bauer, P. (2016). ZINC FINGER OF ARABIDOPSIS THALIANA12 (ZAT12) Interacts with FER-LIKE IRON
779 DEFICIENCY-INDUCED TRANSCRIPTION FACTOR (FIT) Linking Iron Deficiency and Oxidative Stress
780 Responses. *Plant Physiology*, *170*(1), 540–557. https://doi.org/10.1104/pp.15.01589

781 Lehmann, F., & Hardtke, C. S. (2016). Secondary growth of the Arabidopsis hypocotyl—Vascular
782 development in 4 dimensions. *Current Opinion in Plant Biology*, *29*, 9–15.
783 https://doi.org/10.1016/j.pbi.2015.10.011

784 Lemaître, T., Gaufichon, L., Boutet-Mercey, S., Christ, A., & Masclaux-Daubresse, C. (2008).
785 Enzymatic and Metabolic Diagnostic of Nitrogen Deficiency in Arabidopsis thaliana Wassileskija
786 Accession. *Plant and Cell Physiology*, *49*(7), 1056–1065. https://doi.org/10.1093/pcp/pcn081

787 Li, X., Zhang, H., Ai, Q., Liang, G., & Yu, D. (2016). Two bHLH transcription factors, bHLH34 and
788 bHLH104, regulate iron homeostasis in arabidopsis Thaliana. *Plant Physiology*, *170*(4), 2478–2493.
789 https://doi.org/10.1104/pp.15.01827

790 Li, X.-M., Jenke, H., Strauss, S., Bazakos, C., Mosca, G., Lymbouridou, R., Kierzkowski, D.,
791 Neumann, U., Naik, P., Huijser, P., Laurent, S., Smith, R. S., Runions, A., & Tsiantis, M. (2024). Cell-cycle-
792 linked growth reprogramming encodes developmental time into leaf morphogenesis. *Current Biology*,
793 *34*(3), 541-556.e15. https://doi.org/10.1016/j.cub.2023.12.050

794 Lichtblau, D. M., Schwarz, B., Baby, D., Endres, C., Sieberg, C., & Bauer, P. (2022). The Iron
795 Deficiency-Regulated Small Protein Effector FEP3/IRON MAN1 Modulates Interaction of BRUTUS-LIKE1
796 With bHLH Subgroup IVc and POPEYE Transcription Factors. *Frontiers in Plant Science*, *13*(June), 1–22.
797 https://doi.org/10.3389/fpls.2022.930049

798 Long, T. A., Tsukagoshi, H., Busch, W., Lahner, B., Salt, D. E., & Benfey, P. N. (2010). The bHLH
799 Transcription Factor POPEYE Regulates Response to Iron Deficiency in Arabidopsis Roots. *The Plant Cell*,
800 *22*(7), 2219–2236. https://doi.org/10.1105/tpc.110.074096

801 Mai, H.-J., Baby, D., & Bauer, P. (n.d.). *Black sheep, dark horses, and colorful dogs: A review on*
802 *the current state of the Gene Ontology with respect to iron homeostasis in Arabidopsis thaliana*.
803 https://doi.org/10.3389/fpls.2023.1204723

804 Mai, H.-J., Pateyron, S., & Bauer, P. (2016). Iron homeostasis in Arabidopsis thaliana:
805 Transcriptomic analyses reveal novel FIT-regulated genes, iron deficiency marker genes and functional
806 gene networks. *BMC Plant Biology*, *16*(1), 211. https://doi.org/10.1186/s12870-016-0899-9

807 Mendoza-Cózatl, D. G., Xie, Q., Akmakjian, G. Z., Jobe, T. O., Patel, A., Stacey, M. G., Song, L.,
808 Demoin, D. W., Jurisson, S. S., Stacey, G., & Schroeder, J. I. (2014). OPT3 Is a Component of the Iron-
809 Signaling Network between Leaves and Roots and Misregulation of OPT3 Leads to an Over-Accumulation
810 of Cadmium in Seeds. *Molecular Plant*, *7*(9), 1455. https://doi.org/10.1093/MP/SSU067

Muhammad, D., Clark, N. M., Haque, S., Williams, C. M., Sozzani, R., & Long, T. A. (2022). POPEYE intercellular localization mediates cell-specific iron deficiency responses. *Plant Physiology*, *190*(3), 2017–2032. https://doi.org/10.1093/plphys/kiac357

Mukherjee, I., Campbell, N. H., Ash, J. S., & Connolly, E. L. (2006). Expression profiling of the Arabidopsis ferric chelate reductase (FRO) gene family reveals differential regulation by iron and copper. *Planta*, *223*(6), 1178–1190. https://doi.org/10.1007/s00425-005-0165-0

Nam, H.-I., Shahzad, Z., Dorone, Y., Clowez, S., Zhao, K., Bouain, N., Lay-Pruitt, K. S., Cho, H., Rhee, S. Y., & Rouached, H. (2021). Interdependent iron and phosphorus availability controls photosynthesis through retrograde signaling. *Nature Communications*, *12*(1), Article 1. https://doi.org/10.1038/s41467-021-27548-2

Ngigi, M. N., & Bauer, P. (2023). High-Throughput Plant Gene Expression Analysis by 384-Format Reverse Transcription-Quantitative PCR for Investigating Plant Iron Homeostasis. In J. Jeong (Ed.), *Plant Iron Homeostasis: Methods and Protocols* (pp. 1–22). Springer US. https://doi.org/10.1007/978-1-0716-3183-6_1

Nguyen, N. T., Khan, M. A., Castro–Guerrero, N. A., Chia, J.-C., Vatamaniuk, O. K., Mari, S., Jurisson, S. S., & Mendoza-Cozatl, D. G. (2022). Iron Availability within the Leaf Vasculature Determines the Magnitude of Iron Deficiency Responses in Source and Sink Tissues in Arabidopsis. *Plant and Cell Physiology*. https://doi.org/10.1093/PCP/PCAC046

Nguyen, N. T., McInturf, S. A., & Mendoza-Cózatl, D. G. (2016). Hydroponics: A Versatile System to Study Nutrient Allocation and Plant Responses to Nutrient Availability and Exposure to Toxic Elements. *Journal of Visualized Experiments : JoVE*, *113*, 54317. https://doi.org/10.3791/54317

Nooden, L. D., Hillsberg, J. W., & Schneider, M. J. (1996). Induction of leaf senescence in Arabidopsis thaliana by long days through a light-dosage effect. *Physiologia Plantarum*, *96*(3), 491–495. https://doi.org/10.1111/j.1399-3054.1996.tb00463.x

Perea-García, A., Andrés-Bordería, A., Vera-Sirera, F., Pérez-Amador, M. A., Puig, S., & Peñarrubia, L. (2020). *Deregulated High Affinity Copper Transport Alters Iron Homeostasis in Arabidopsis*. https://doi.org/10.3389/fpls.2020.01106

Pottier, M., Dumont, J., Masclaux-Daubresse, C., & Thomine, S. (2019a). Autophagy is essential for optimal translocation of iron to seeds in Arabidopsis. *Journal of Experimental Botany*, *70*(3), 859–869. https://doi.org/10.1093/jxb/ery388

Pottier, M., Dumont, J., Masclaux-Daubresse, C., & Thomine, S. (2019b). Autophagy is essential for optimal translocation of iron to seeds in Arabidopsis. *Journal of Experimental Botany*, *70*(3), 859–869. https://doi.org/10.1093/jxb/ery388

Pu, M. N., & Liang, G. (2023). The transcription factor POPEYE negatively regulates the expression of bHLH Ib genes to maintain iron homeostasis. *Journal of Experimental Botany*, *74*(8), 2754–2767. https://doi.org/10.1093/jxb/erad057

Rai, S., Singh, P. K., Mankotia, S., Swain, J., & Satbhai, S. B. (2021). Iron homeostasis in plants and its crosstalk with copper, zinc, and manganese. *Plant Stress*, *1*, 100008. https://doi.org/10.1016/j.stress.2021.100008

Rodríguez-Celma, J., Connorton, J. M., Kruse, I., Green, R. T., Franceschetti, M., Chen, Y. T., Cui, Y., Ling, H. Q., Yeh, K. C., & Balk, J. (2019). Arabidopsis BRUTUS-LIKE E3 ligases negatively regulate iron uptake by targeting transcription factor FIT for recycling. *Proceedings of the National Academy of Sciences of the United States of America*, *116*(35), 17584–17591. https://doi.org/10.1073/pnas.1907971116

Sági-Kazár, M., Solymosi, K., & Solti, Á. (2022). Iron in leaves: Chemical forms, signalling, and in-cell distribution. *Journal of Experimental Botany*, *73*(6), 1717–1734. https://doi.org/10.1093/jxb/erac030

Saini, K., Dwivedi, A., & Ranjan, A. (2022). High temperature restricts cell division and leaf size by coordination of PIF4 and TCP4 transcription factors. *Plant Physiology*, *190*(4), 2380–2397. https://doi.org/10.1093/plphys/kiac345

Schuler, M. (2011). *The role of nicotianamine in the metal homeostasis of Arabidopsis thaliana*.

Schuler, M., Rellán-Álvarez, R., Fink-Straube, C., Abadía, J., & Bauera, P. (2012). Nicotianamine functions in the phloem-based transport of iron to sink organs, in pollen development and pollen tube growth in Arabidopsis. *Plant Cell*, *24*(6), 2380–2400. https://doi.org/10.1105/tpc.112.099077

Schwarz, B., & Bauer, P. (2020). FIT, a regulatory hub for iron deficiency and stress signaling in roots, and FIT-dependent and -independent gene signatures. *Journal of Experimental Botany*, *71*(5), 1694–1705. https://doi.org/10.1093/jxb/eraa012

Sheng, H., Jiang, Y., Rahmati, M., Chia, J.-C., Dokuchayeva, T., Kavulych, Y., Zavodna, T.-O., Mendoza, P. N., Huang, R., Smieshka, L. M., Miller, J., Woll, A. R., Terek, O. I., Romanyuk, N. D., Piñeros, M., Zhou, Y., & Vatamaniuk, O. K. (2021). YSL3-mediated copper distribution is required for fertility, seed size and protein accumulation in Brachypodium. *Plant Physiology*, *186*(1), 655–676. https://doi.org/10.1093/plphys/kiab054

Sperotto, R. A., Vasconcelos, M. W., Grusak, M. A., & Fett, J. P. (2012). *Effects of different Fe supplies on mineral partitioning and remobilization during the reproductive development of rice (Oryza sativa L.)*. https://pmc.ncbi.nlm.nih.gov/articles/PMC4883723/

Stacey, M. G., Patel, A., McClain, W. E., Mathieu, M., Remley, M., Rogers, E. E., Gassmann, W., Blevins, D. G., & Stacey, G. (2008). The Arabidopsis AtOPT3 Protein Functions in Metal Homeostasis and Movement of Iron to Developing Seeds. *Plant Physiology*, *146*(2), 589. https://doi.org/10.1104/PP.107.108183

Swartz, L. G., Liu, S., Dahlquist, D., Kramer, S. T., Walter, E. S., McInturf, S. A., Bucksch, A., & Mendoza-Cózatl, D. G. (2023). OPEN leaf: An open-source cloud-based phenotyping system for tracking dynamic changes at leaf-specific resolution in Arabidopsis. *The Plant Journal*, *116*(6), 1600–1616. https://doi.org/10.1111/tpj.16449

Tanabe, N., Noshi, M., Mori, D., Nozawa, K., Tamoi, M., & Shigeoka, S. (2018). The basic helix-loop-helix transcription factor, bHLH11 functions in the iron-uptake system in Arabidopsis thaliana. *Journal of Plant Research*, *132*(1), Article 1. https://doi.org/10.1007/s10265-018-1068-z

Tanabe, N., Noshi, M., Mori, D., Nozawa, K., Tamoi, M., & Shigeoka, S. (2019). The basic helix-loop-helix transcription factor, bHLH11 functions in the iron-uptake system in Arabidopsis thaliana. *Journal of Plant Research*, *132*(1), 93–105. https://doi.org/10.1007/s10265-018-1068-z

Tissot, N., Robe, K., Gao, F., Grant-Grant, S., Boucherez, J., Bellegarde, F., Maghiaoui, A., Marcelin, R., Izquierdo, E., Benhamed, M., Martin, A., Vignols, F., Roschzttardtz, H., Gaymard, F., Briat, J. F., & Dubos, C. (2019). Transcriptional integration of the responses to iron availability in Arabidopsis by the bHLH factor ILR3. *New Phytologist*, *223*(3), 1433–1446. https://doi.org/10.1111/nph.15753

Trofimov, K., Ivanov, R., Eutebach, M., Acaroglu, B., Mohr, I., Bauer, P., & Brumbarova, T. (2019). Mobility and localization of the iron deficiency-induced transcription factor bHLH039 change in the presence of FIT. *Plant Direct*, *3*(12), e00190. https://doi.org/10.1002/pld3.190

Tsukaya, H. (2005). Leaf shape: Genetic controls and environmental factors. *The International Journal of Developmental Biology*, *49*(5–6), 547–555. https://doi.org/10.1387/ijdb.041921ht

Tsukaya, H., Shoda, K., Kim, G. T., & Uchimiya, H. (2000). Heteroblasty in Arabidopsis thaliana (L.) Heynh. *Planta*, *210*(4), 536–542. https://doi.org/10.1007/s004250050042

Wang, W., Luo, L., Shi, H., Song, Y., Wang, J., Chen, C., Shen, Z., Rouached, H., & Zheng, L. (2024). The transcription factor OsSPL9 endows rice with copper deficiency resilience. *Journal of Experimental Botany*, *75*(18), 5909–5922. https://doi.org/10.1093/jxb/erae273

Wang, Y. (n.d.). *MIR156 Participates in Iron Homeostasis Through Targeting SPL9/SPL15 in Arabidopsis Thaliana*.

Waters, B. M., & Armbrust, L. C. (2013). Optimal copper supply is required for normal plant iron deficiency responses. *Plant Signaling & Behavior*, *8*(12), e26611. https://doi.org/10.4161/psb.26611

Waters, B. M., & Grusak, M. A. (2008a). Whole-plant mineral partitioning throughout the life cycle in Arabidopsis thaliana ecotypes Columbia, Landsberg erecta, Cape Verde Islands, and the mutant line ysl1ysl3. *New Phytologist*, *177*(2), 389–405. https://doi.org/10.1111/j.1469-8137.2007.02288.x

Waters, B. M., & Grusak, M. A. (2008b). Whole-plant mineral partitioning throughout the life cycle in Arabidopsis thaliana ecotypes Columbia, Landsberg erecta, Cape Verde Islands, and the mutant line ysl1ysl3. *New Phytologist*, *177*(2), 389–405. https://doi.org/10.1111/J.1469-8137.2007.02288.X

Waters, B. M., Uauy, C., Dubcovsky, J., & Grusak, M. A. (2009). Wheat (Triticum aestivum) NAM proteins regulate the translocation of iron, zinc, and nitrogen compounds from vegetative tissues to grain. *Journal of Experimental Botany*, *60*(15), 4263–4274. https://doi.org/10.1093/jxb/erp257

Wu, G., Park, M. Y., Conway, S. R., Wang, J.-W., Weigel, D., & Poethig, R. S. (2009). The Sequential Action of miR156 and miR172 Regulates Developmental Timing in *Arabidopsis*. *Cell*, *138*(4), 750–759. https://doi.org/10.1016/j.cell.2009.06.031

Wunderling, A., Ripper, D., Barra-Jimenez, A., Mahn, S., Sajak, K., Targem, M. B., & Ragni, L. (2018). *A molecular framework to study periderm formation in Arabidopsis*. https://doi.org/10.1111/nph.15128

Xu, M., Hu, T., Zhao, J., Park, M.-Y., Earley, K. W., Wu, G., Yang, L., & Poethig, R. S. (2016). Developmental Functions of miR156-Regulated SQUAMOSA PROMOTER BINDING PROTEIN-LIKE (SPL) Genes in Arabidopsis thaliana. *PLOS Genetics*, *12*(8), e1006263. https://doi.org/10.1371/journal.pgen.1006263

Zhai, Z., Gayomba, S. R., Jung, H.-I., Vimalakumari, N. K., Piñeros, M., Craft, E., Rutzke, M. A., Danku, J., Lahner, B., Punshon, T., Guerinot, M. L., Salt, D. E., Kochian, L. V., & Vatamaniuk, O. K. (2014). *OPT3 Is a Phloem-Specific Iron Transporter That Is Essential for Systemic Iron Signaling and Redistribution of Iron and Cadmium in Arabidopsis*. https://doi.org/10.1105/tpc.114.123737

Zhang, J., Liu, B., Li, M., Feng, D., Jin, H., Wang, P., Liu, J., Xiong, F., Wang, J., & Wang, H.-B. (2015). The bHLH Transcription Factor bHLH104 Interacts with IAA-LEUCINE RESISTANT3 and Modulates Iron Homeostasis in Arabidopsis. *The Plant Cell*, *27*(3), 787–805. https://doi.org/10.1105/tpc.114.132704

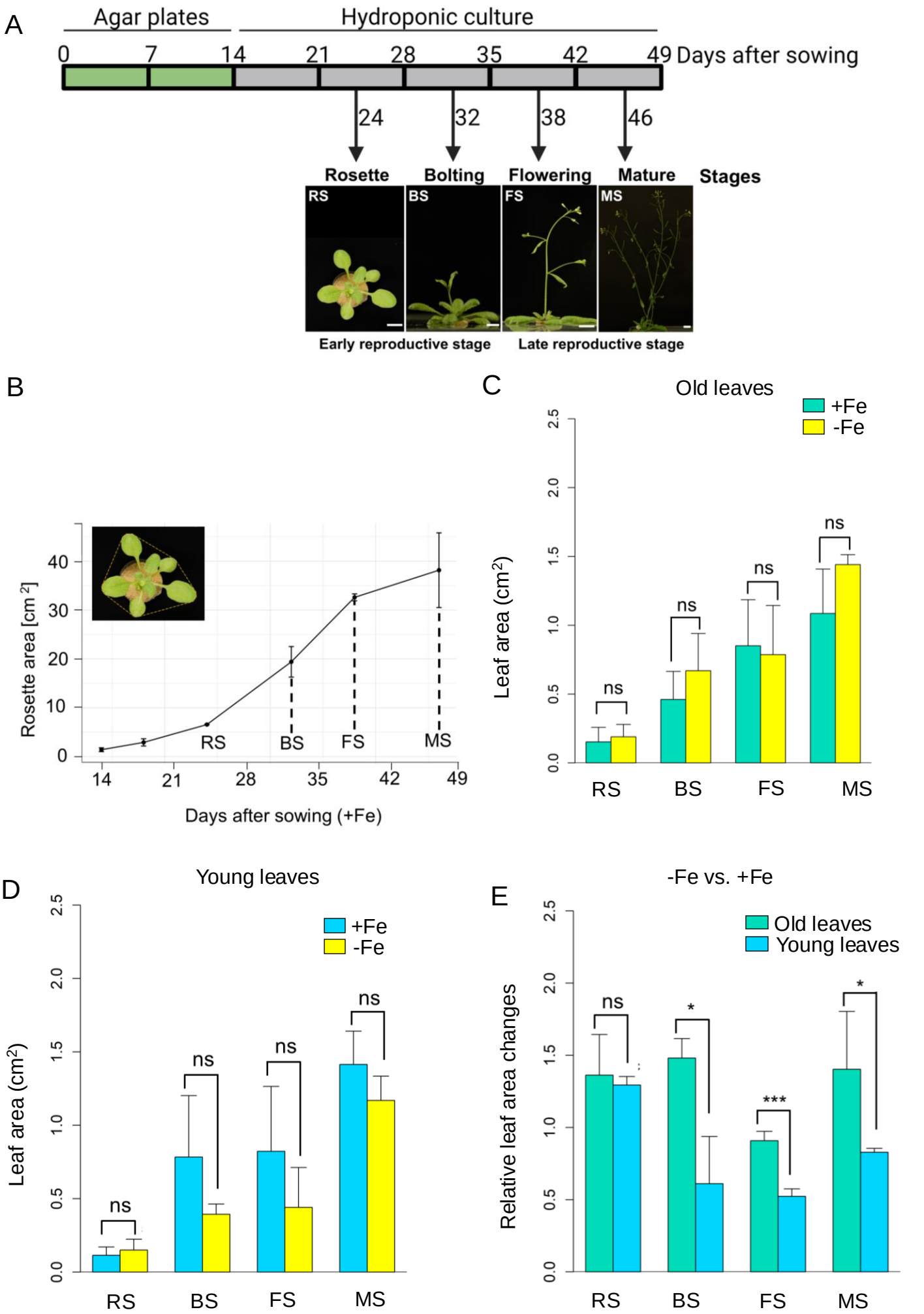
A
Agar plates
Hydroponic culture
0
7
14
21
28
35
42
49
Days after sowing
24
32
38
46
Rosette
Bolting
Flowering
Mature
Stages
RS
BS
FS
MS
Early reproductive stage
Late reproductive stage
B
Rosette area [cm 2]
Days after sowing (+Fe)
RS
BS
FS
MS
C
Old leaves
+Fe
-Fe
Leaf area (cm2)
ns
RS
BS
FS
MS
D
Young leaves
+Fe
-Fe
Leaf area (cm2)
ns
RS
BS
FS
MS
E
-Fe vs. +Fe
Old leaves
Young leaves
Relative leaf area changes
ns
*
***
*
RS
BS
FS
MS

Figure 1. Growth dynamics during progression of the *Arabidopsis* life cycle. (A) Overview of experimental setup and reproductive growth stages selected for analysis of *Arabidopsis thaliana*. Seedlings were germinated on Hoagland agar plates before transplanting to standard hydroponic media with 25 µM Fe (+Fe) for growth to the four selected stages under long-day conditions; rosette stage (RS), bolting stage (BS), flowering stage (FS) and mature silique stage (MS) before further analysis, scale bar = 1cm. Further details on the reproductive growth stages in Figure S1A, B. (B) Rosette area increase of plants continuously grown on media with +Fe until the mature stage. Rosette area included all leaves forming around the canopy plus their petioles (n = 2-8). (C-D) Absolute leaf areas of old and young leaves at +Fe and –Fe, respectively. Plants were transferred to +Fe and –Fe conditions for 3 days at the indicated growth stages. Old and young leaves harvested for analysis are described in Figure S1C. (E) Relative changes in leaf area sizes of old and young leaves under –Fe compared to +Fe conditions at the stages RS to MS. Data in (C-D) represent average values of biological replicates (n=5). Error bars show ± SD. Statistical analysis was done by Student's t-test ($p < 0.05$).

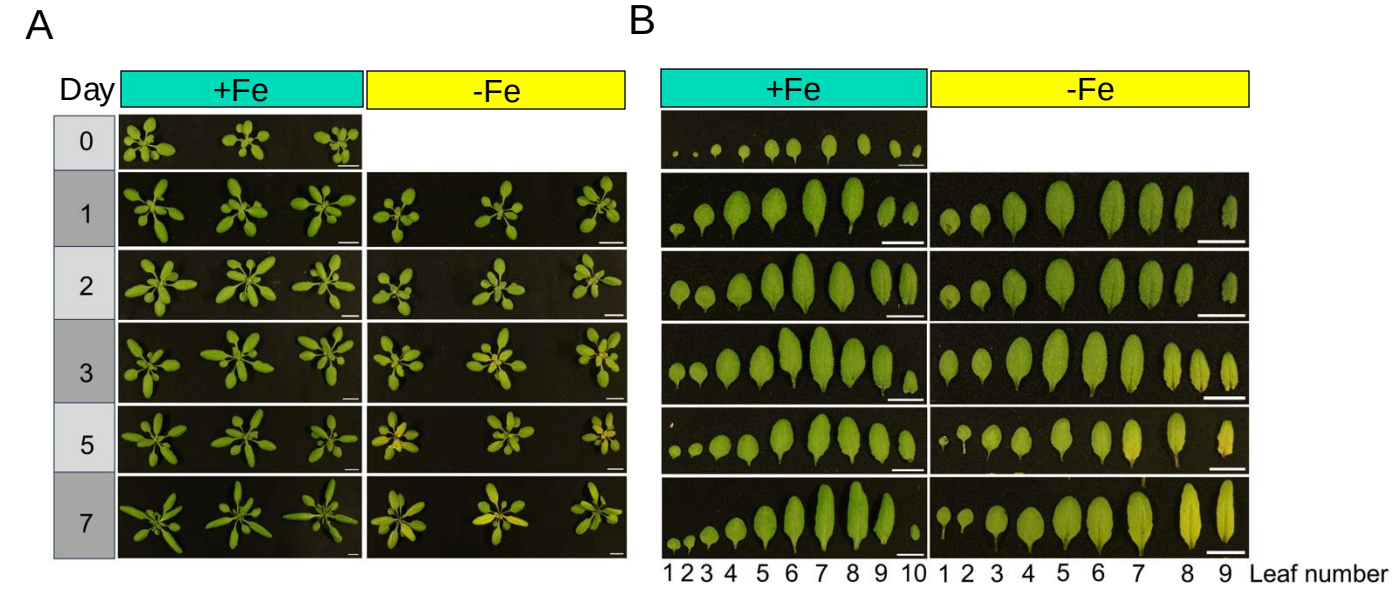
A
Day
+Fe
-Fe
0
1
2
3
5
7
B
+Fe
-Fe
1 2 3 4 5 6 7 8 9 10 1 2 3 4 5 6 7 8 9 Leaf number

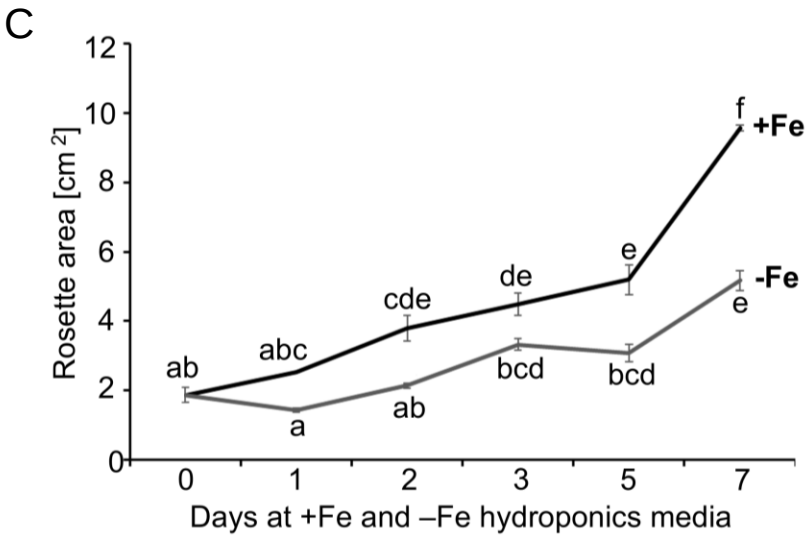
C
Rosette area [cm 2]
12
10
8
6
4
2
0
0
1
2
3
5
7
Days at +Fe and –Fe hydroponics media
+Fe
-Fe
ab
abc
cde
de
e
f
a
ab
bcd
bcd
e

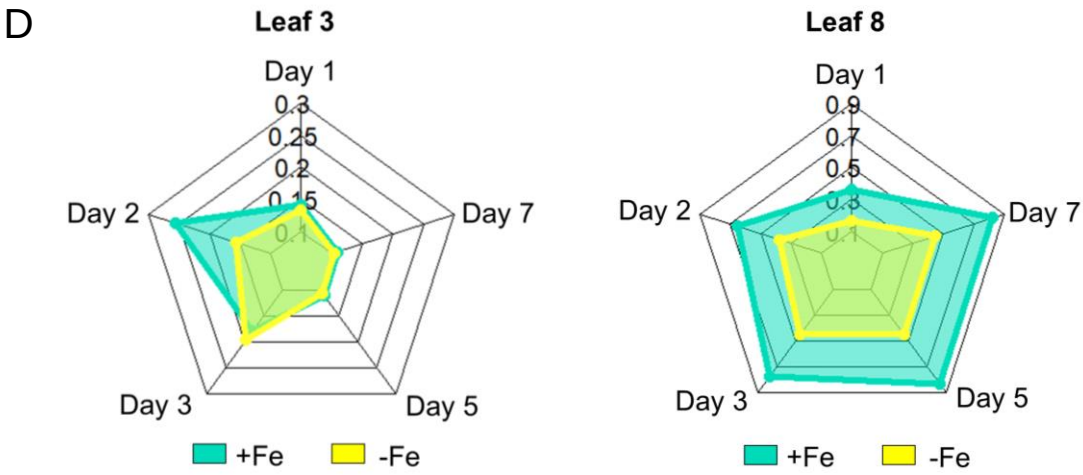
D
Leaf 3
Day 1
Day 2
Day 3
Day 5
Day 7
0.3
0.25
0.2
0.15
0.1
+Fe
-Fe
Leaf 8
Day 1
Day 2
Day 3
Day 5
Day 7
0.9
0.7
0.5
0.3
0.1
+Fe
-Fe

Figure 2. Leaf-by-leaf analysis of *Arabidopsis thaliana* at the rosette stage (RS). (A) At the RS, plants were transferred to respective Fe sufficient (+Fe) or deficient (-Fe) Hoagland media solutions and growth recorded from day 0 till day 7. (B) Leaf images of leaf 1 (L1) to 10 (L10) at the two Fe conditions, as indicated. (C) Cumulative rosette area as recorded from (A). Data represent means of biological replicates (*n*=3). Error bars represent ± SD. Statistical analysis was done using one-way ANOVA and Tukey's HSD test. Means followed by the same letter are not significantly different ($p < 0.05$). (D) Radial charts showing the leaf sizes of leaf 3 and 8 after exposure to either +Fe (control) or –Fe conditions from day 1 to day 7. Radial charts were plotted in R Studio using "fsmb" package. Plants were grown for 3 weeks before culturing in either +Fe or -Fe conditions.

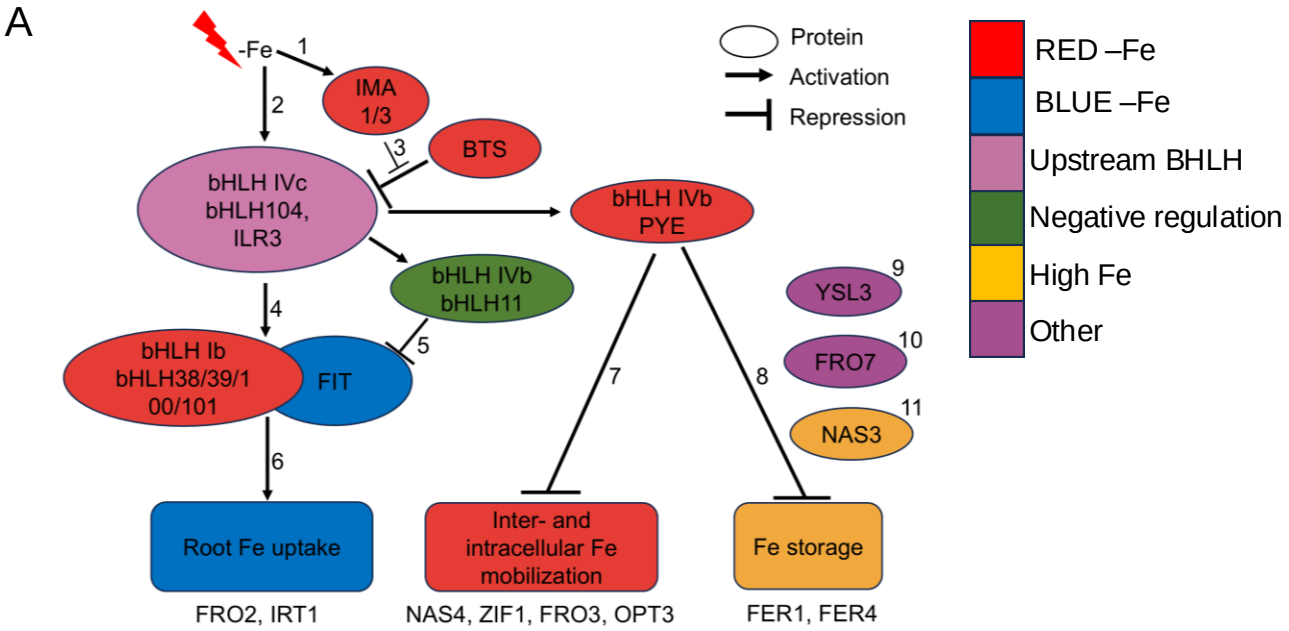
A
-Fe
1
2
IMA 1/3
3
BTS
bHLH IVc bHLH104, ILR3
bHLH IVb PYE
bHLH IVb bHLH11
4
5
bHLH Ib bHLH38/39/100/101
FIT
6
7
8
9
YSL3
10
FRO7
11
NAS3
Protein
Activation
Repression
RED –Fe
BLUE –Fe
Upstream BHLH
Negative regulation
High Fe
Other
Root Fe uptake
Inter- and intracellular Fe mobilization
Fe storage
FRO2, IRT1
NAS4, ZIF1, FRO3, OPT3
FER1, FER4

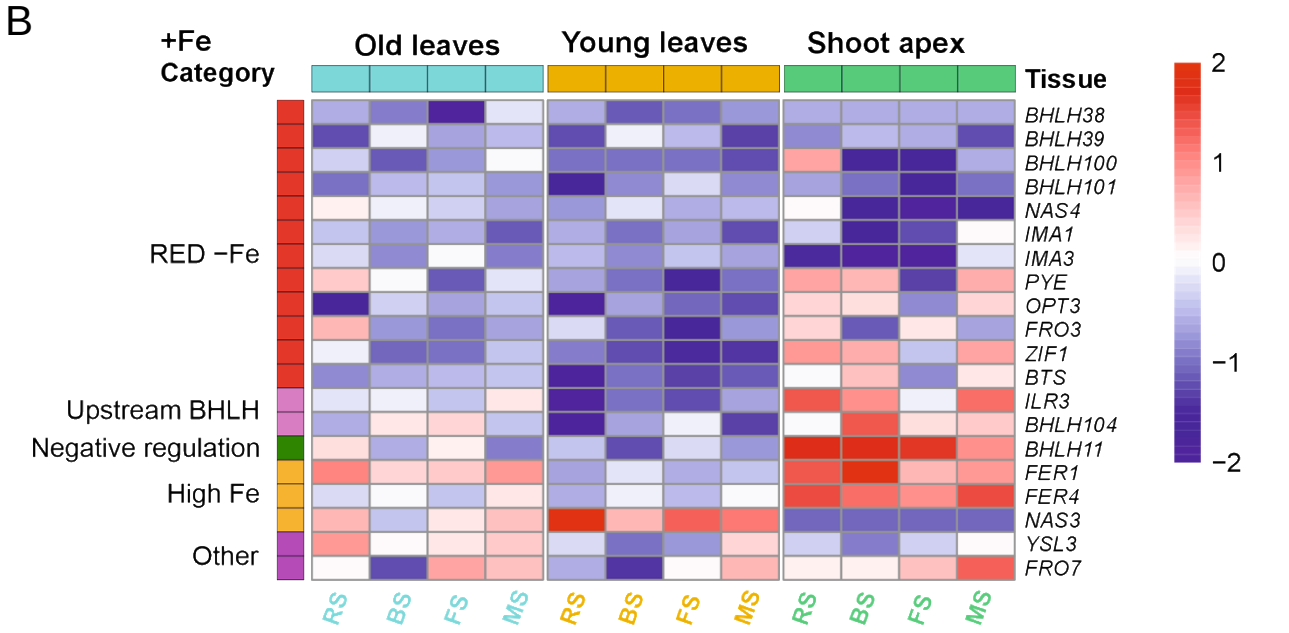
B
+Fe Category
Old leaves
Young leaves
Shoot apex
Tissue
RED −Fe
Upstream BHLH
Negative regulation
High Fe
Other
BHLH38
BHLH39
BHLH100
BHLH101
NAS4
IMA1
IMA3
PYE
OPT3
FRO3
ZIF1
BTS
ILR3
BHLH104
BHLH11
FER1
FER4
NAS3
YSL3
FRO7
RS
BS
FS
MS
2
1
0
−1
−2

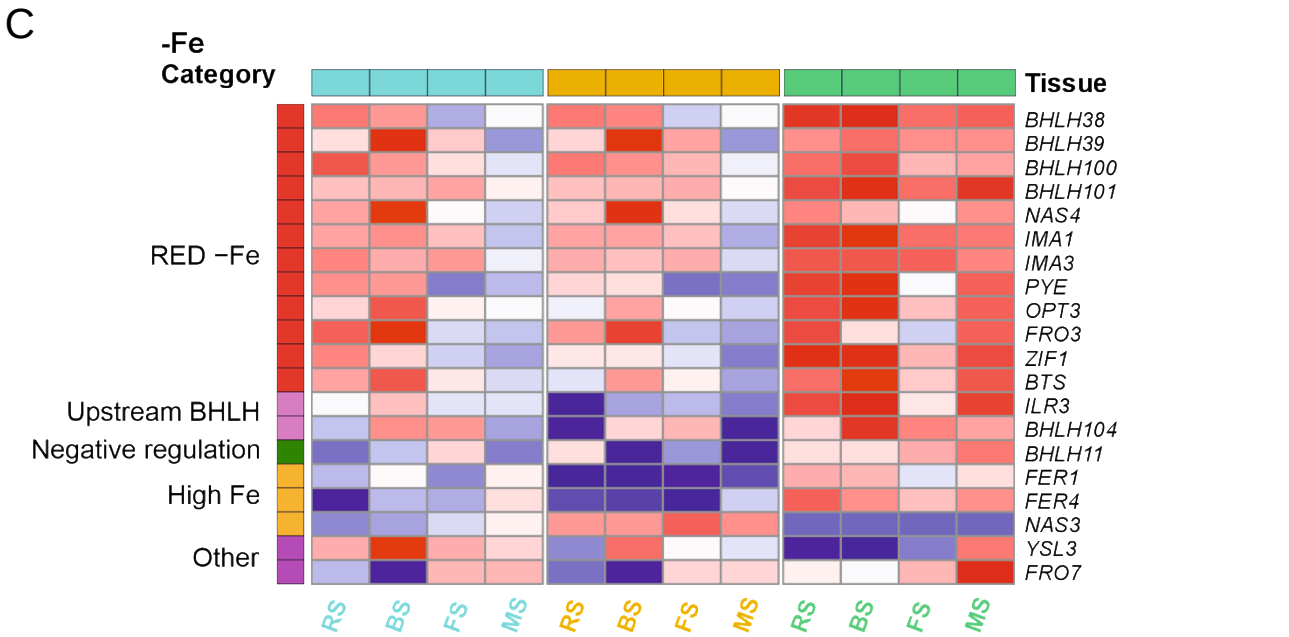
C
-Fe Category
Tissue
RED −Fe
Upstream BHLH
Negative regulation
High Fe
Other
BHLH38
BHLH39
BHLH100
BHLH101
NAS4
IMA1
IMA3
PYE
OPT3
FRO3
ZIF1
BTS
ILR3
BHLH104
BHLH11
FER1
FER4
NAS3
YSL3
FRO7
RS
BS
FS
MS

Figure 3. Gene expression analysis of selected Fe homeostasis genes. (A) Schematic illustration showing connections and functions of Fe homeostasis genes used in gene expression analysis. Represented is the Fe-regulated transcriptional cascade and multiple layers of co-expressed genes involved in plant Fe homeostasis. Exemplary references: [1](Kobayashi et al., 2021), [2](Zhang et al., 2015), [3](Lichtblau et al., 2022), [4](Li et al., 2016), [5](Tanabe et al., 2018), [6](Trofimov et al., 2019), [7](Long et al., 2010), [8](Tissot et al., 2019), [9](Chu et al., 2010), [10](Mukherjee et al., 2006), [11](Schuler et al., 2012). (B-C) Heatmaps showing the absolute expression profiles of 20 selected Fe homeostasis genes in old leaves, young leaves, and inflorescence shoot apices after exposure to +Fe and –Fe for 3 days. Plants were grown to the various stages, as indicated, before transfer to either Fe solutions. The growth stages RS, BS, FS and MS correspond to rosette stage, bolting stage, flowering stage and mature stage, respectively. Heatmaps were generated in R studio version 4.4.1 using calculated z-scores of normalized gene expression values of each gene across tissues for both +Fe and –Fe. Category annotations are displayed on the left side of the heatmap, with tissue-type annotations displayed on the top. The colour scale ranges from -2 to 2 to represent the variation in gene expression. Red colours represent gene up-regulation, and blue colours represent gene down-regulation, $p < 0.05$ ($n = 3$).

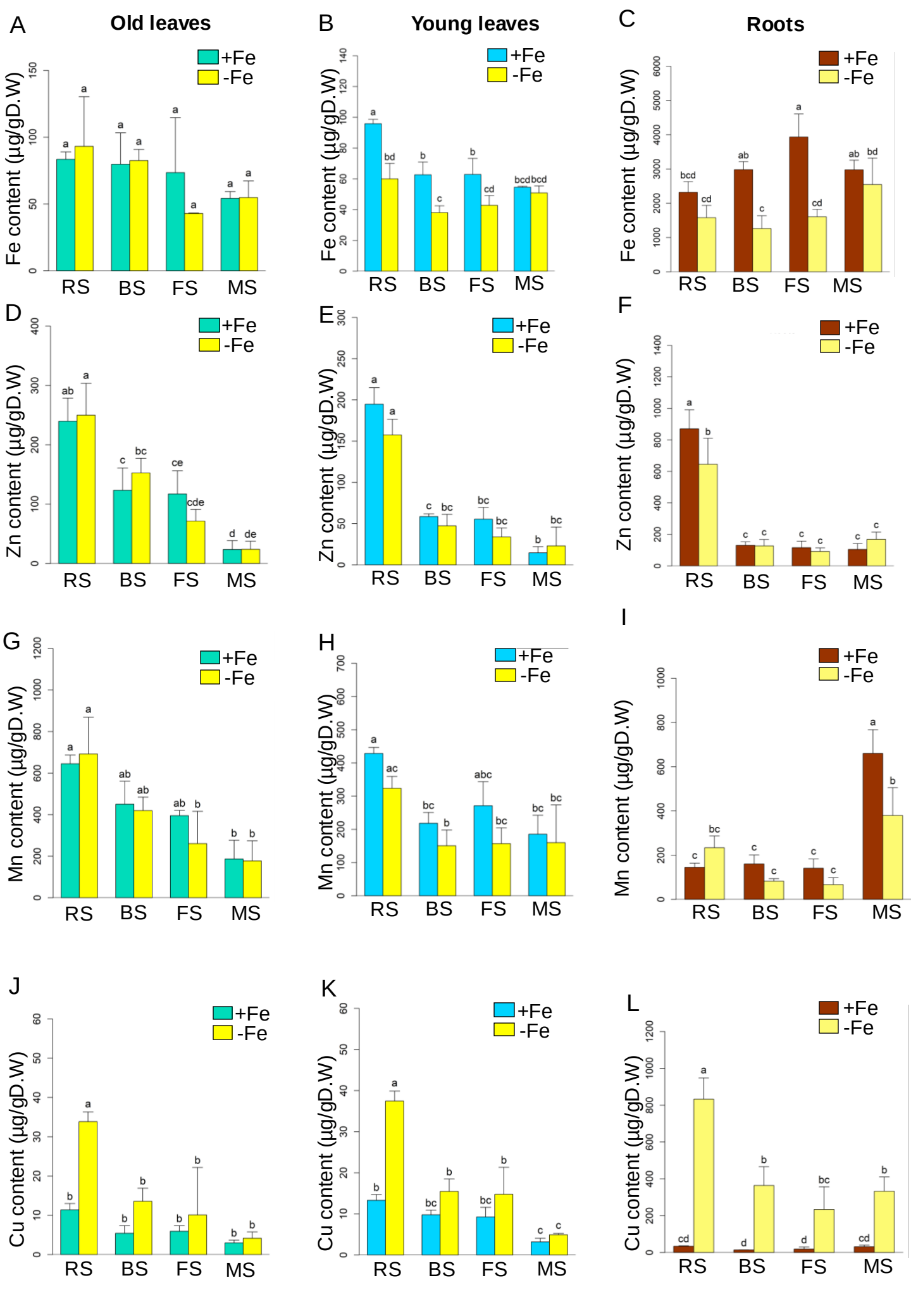
A
Old leaves
B
Young leaves
C
Roots
+Fe
-Fe
Fe content (µg/gD.W)
Zn content (µg/gD.W)
Mn content (µg/gD.W)
Cu content (µg/gD.W)
RS
BS
FS
MS
D
E
F
G
H
I
J
K
L

Figure 4. Ionomic analysis of leaves and roots. Fe (A-C), Zn (D-F), Mn (G-I), and Cu (J-L) content per dry weight (D.W.) in old leaves, young leaves and roots of plants grown at 25 µM Fe (+Fe) or 0 µM Fe (–Fe) conditions and at the four growth stages; RS, BS, FS and MS. Plants were exposed to 3 days of +Fe or –Fe before sample collection. Data represents mean of three biological replicates (n = 3). Error bars represent ± SD. Letters on top of each bar show level of significance according to Tukey's HSD test, $p < 0.05$.

A

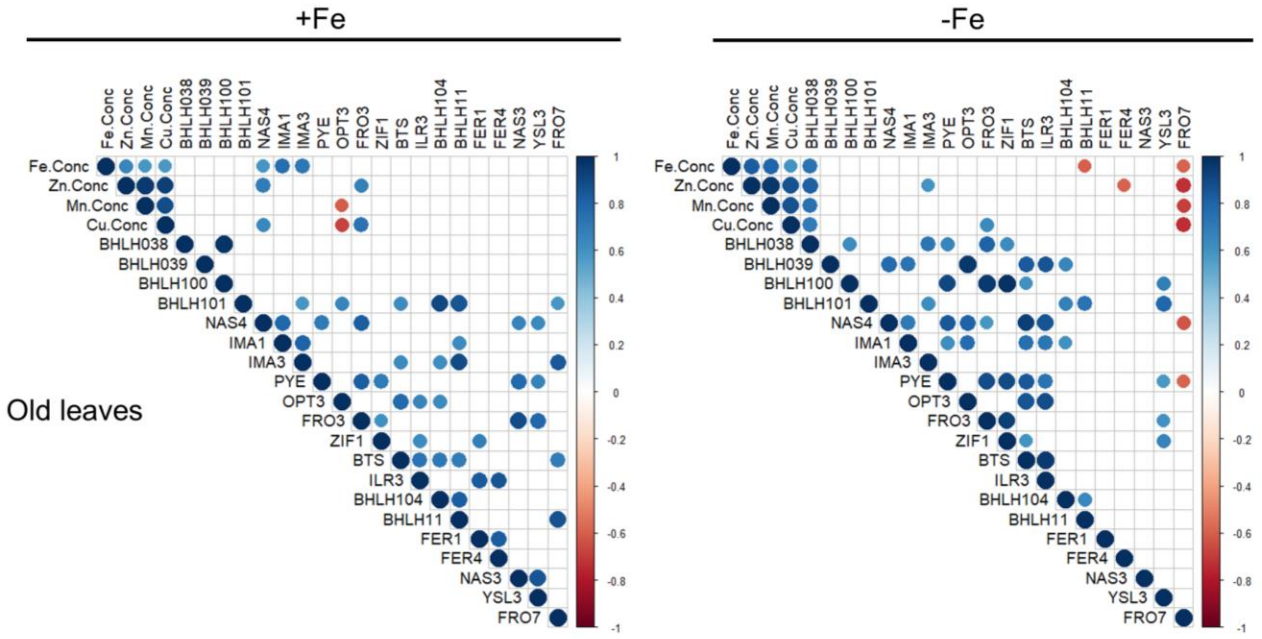

B

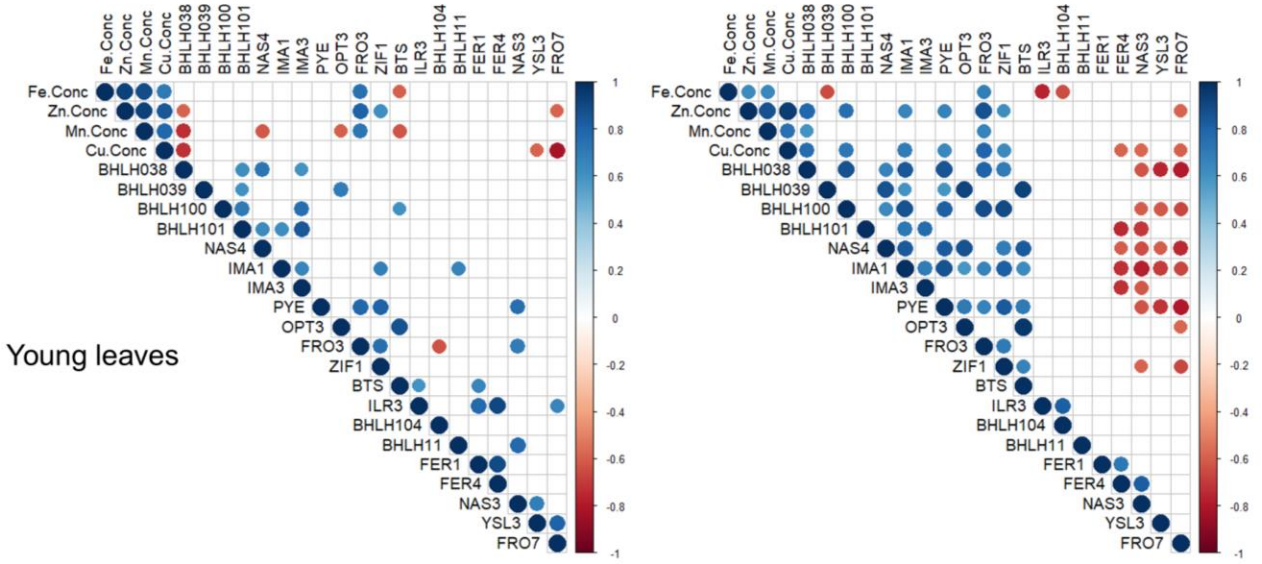

C

	Mineral to mineral correlations				Mineral to gene correlations				Gene to gene correlations			
	OL		YL		OL		YL		OL		YL	
	+Fe	-Fe	+Fe	-Fe	+Fe	-Fe	+Fe	-Fe	+Fe	-Fe	+Fe	-Fe
Positive	6	6	6	5	7	6	4	15	39	44	29	39
Negative	-	-	-	-	2	6	10	7	-	2	1	24

Figure 5. Correlation analysis between gene expression changes and ionomic contents. Correlations were performed with data from old leaves (A), and young leaves (B) at +Fe (right side) and -Fe (left side) conditions. Analysis was done using averages of normalized gene expression values and mineral concentrations of Fe (Fe Conc.), Zn (Zn Conc.), Mn (Mn Conc.) and Cu (Cu Conc.) across all four stages RS, BS, FS, and MS. Color scale represents Pearson's correlation coefficients normalized in the range between -1 to 1, whereby -1 is negative correlations and 1 is positive correlations calculated between genes and mineral content pair. Significant correlations at $p < 0.05$ are displayed in the diagram. (C) Summary table showing number of correlations between either mineral-to-mineral content, mineral content to gene expression level and correlation of gene gene-to-gene expression level in old and young leaves. Numbers show total number of positive and negative correlations at both +Fe and –Fe conditions.

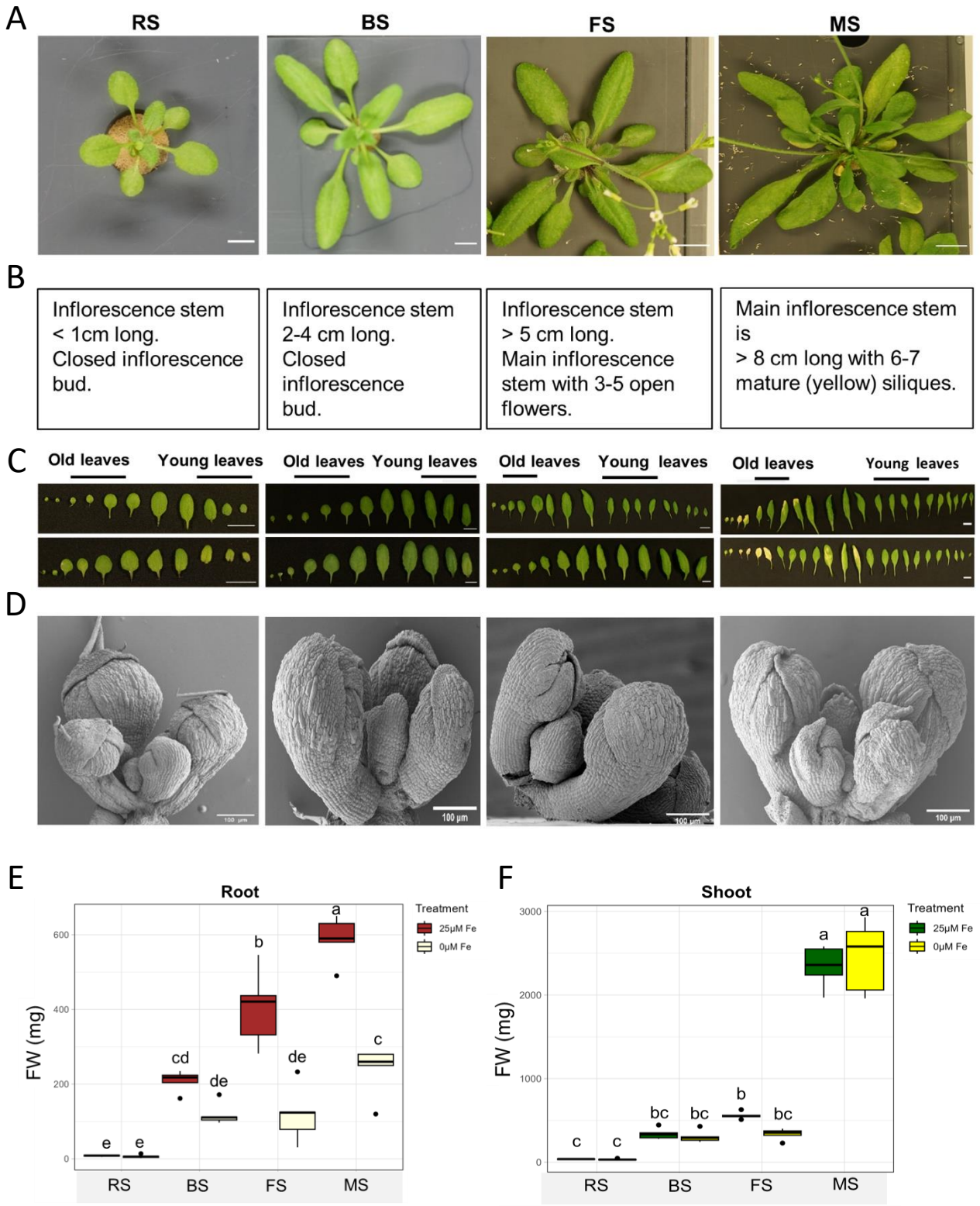

Figure S1. Materials collected from *Arabidopsis thaliana* plants. (A) Top view of plants with their rosette leaves at each stage, scale bar = 1cm. (B) Descriptions of the growth stages distinguishing phenotypes as described by (Boyes et al., 2001). (C) Old (left) and young (right) leaves collected from plants at the respective stages under +Fe (control) and –Fe after 3 days, scale bar = 1cm. (D) Scanning electron microscopy images of inflorescence shoot apical meristems dissected from the main stems of plants at the rosette to mature stages, scale bar = 100 µm. (E-F) Root and shoot fresh weights of plants grown to RS, BS, FS, and MS and transferred to hydroponic media with +Fe or -Fe for 3 days. Data represents mean of three biological replicates (n = 3). Error bars represent ± SD.

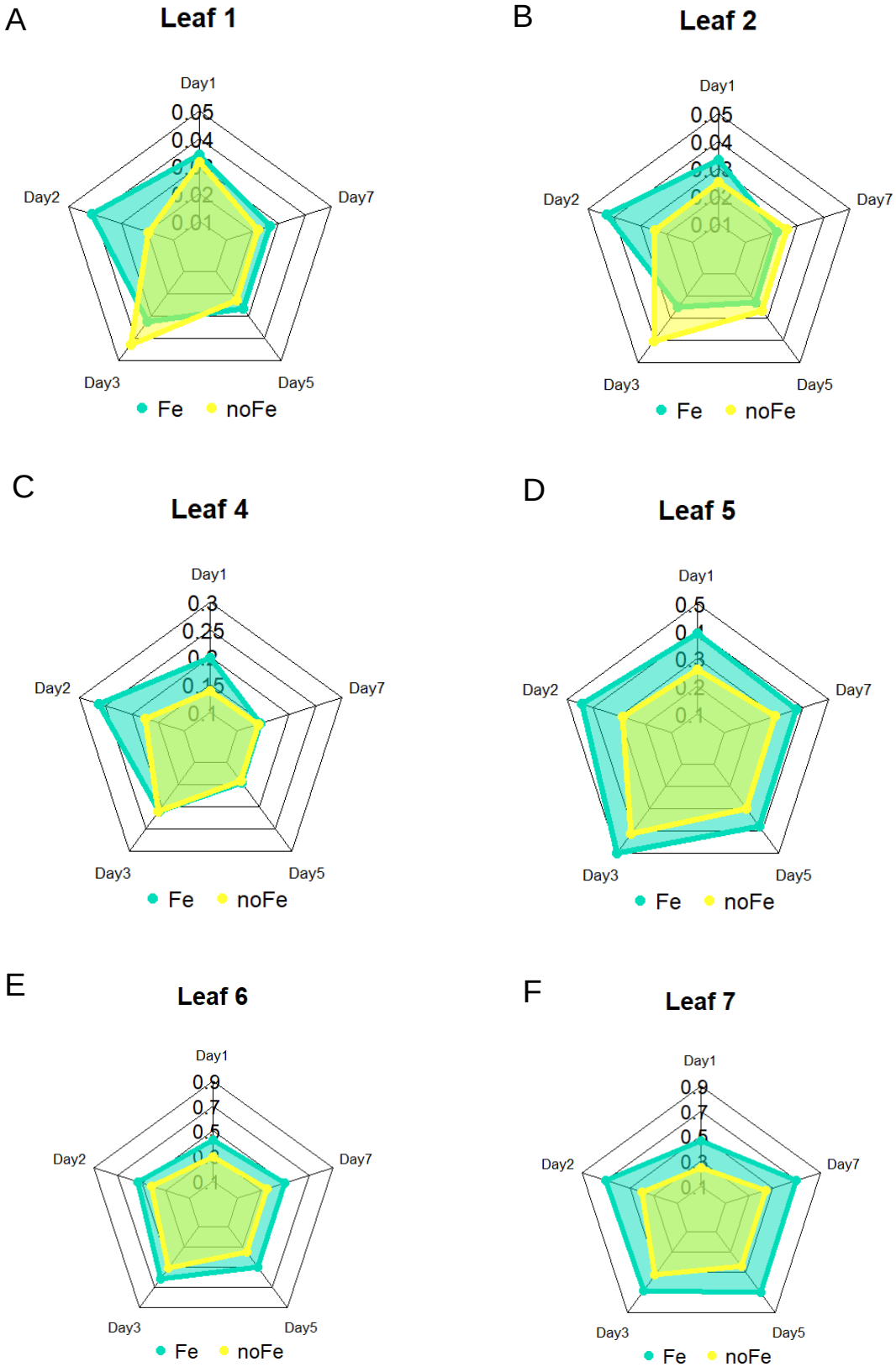

Figure S2. Radial charts showing the leaf sizes at +Fe and -Fe**.** (A-F) Individual leaf sizes of plants (L1, L2, L4, L5, L6 and L7) at RS after exposure to either Fe sufficient (+Fe) or deficient (-Fe) conditions from day 1 to day 7, as indicated. Data represents the average of biological replicates (*n*=3). Radial charts were plotted in R Studio using "fsmb" package.

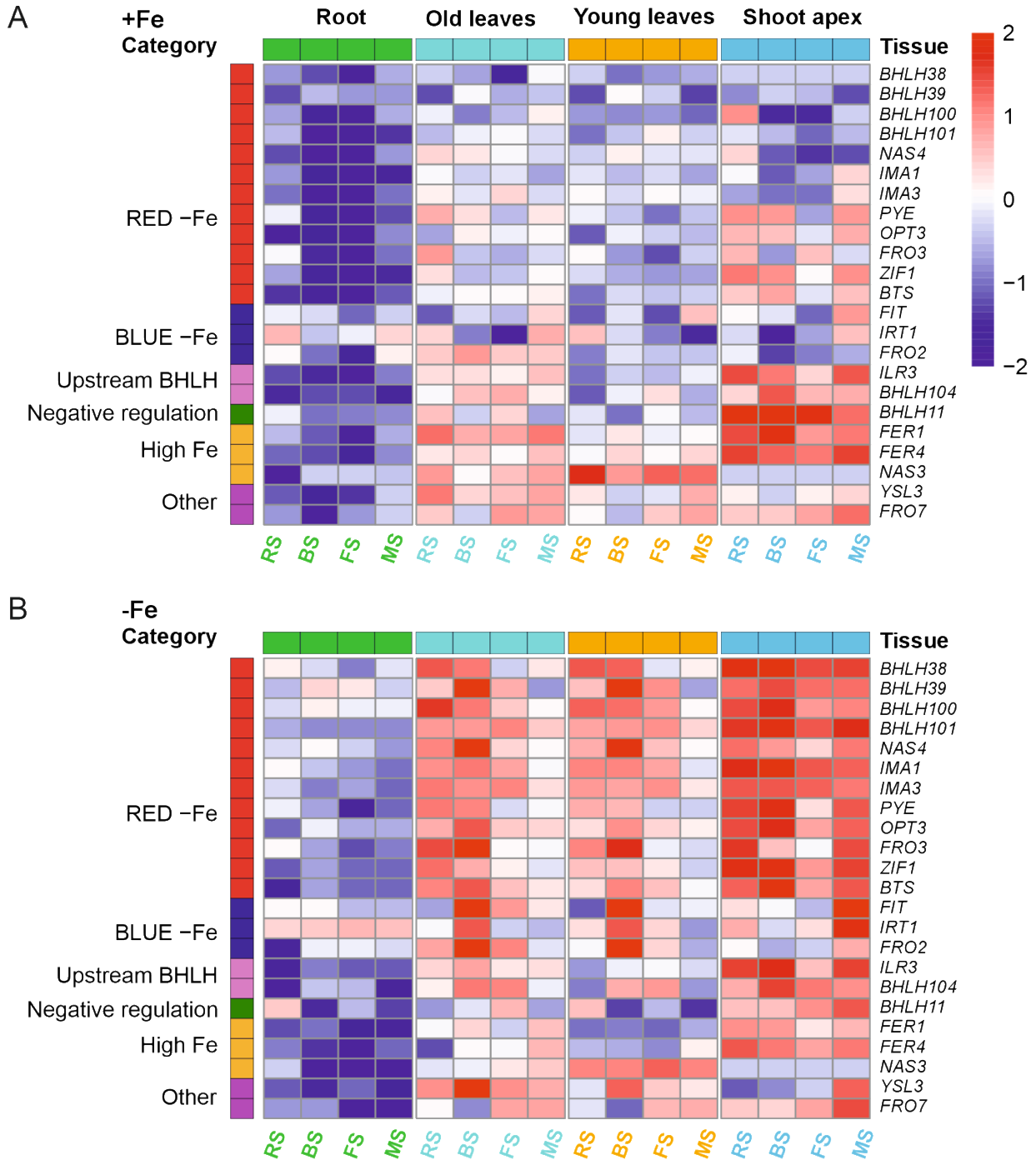

Figure S3. Gene expression analysis of selected Fe homeostasis genes in leaves, shoot apices and roots. (A-B) Heatmaps showing the absolute expression profile of Fe-response markers in roots, old leaves, young leaves, and inflorescence shoot apex +Fe and –Fe respectively, for 3 days at RS, BS, FS and MS. Heatmaps were generated in R studio version 4.4.1 using calculated z-scores of normalized gene expression values of each gene across tissues for both +Fe and –Fe. Category annotations are displayed on the left side of the heatmap, with tissue-type annotations displayed on the top. The colour scale ranges from -2 to 2 to represent the variation in gene expression. Red colours represent gene up-regulation, and blue colours represent gene down-regulation, $p < 0.05$ ($n = 3$).

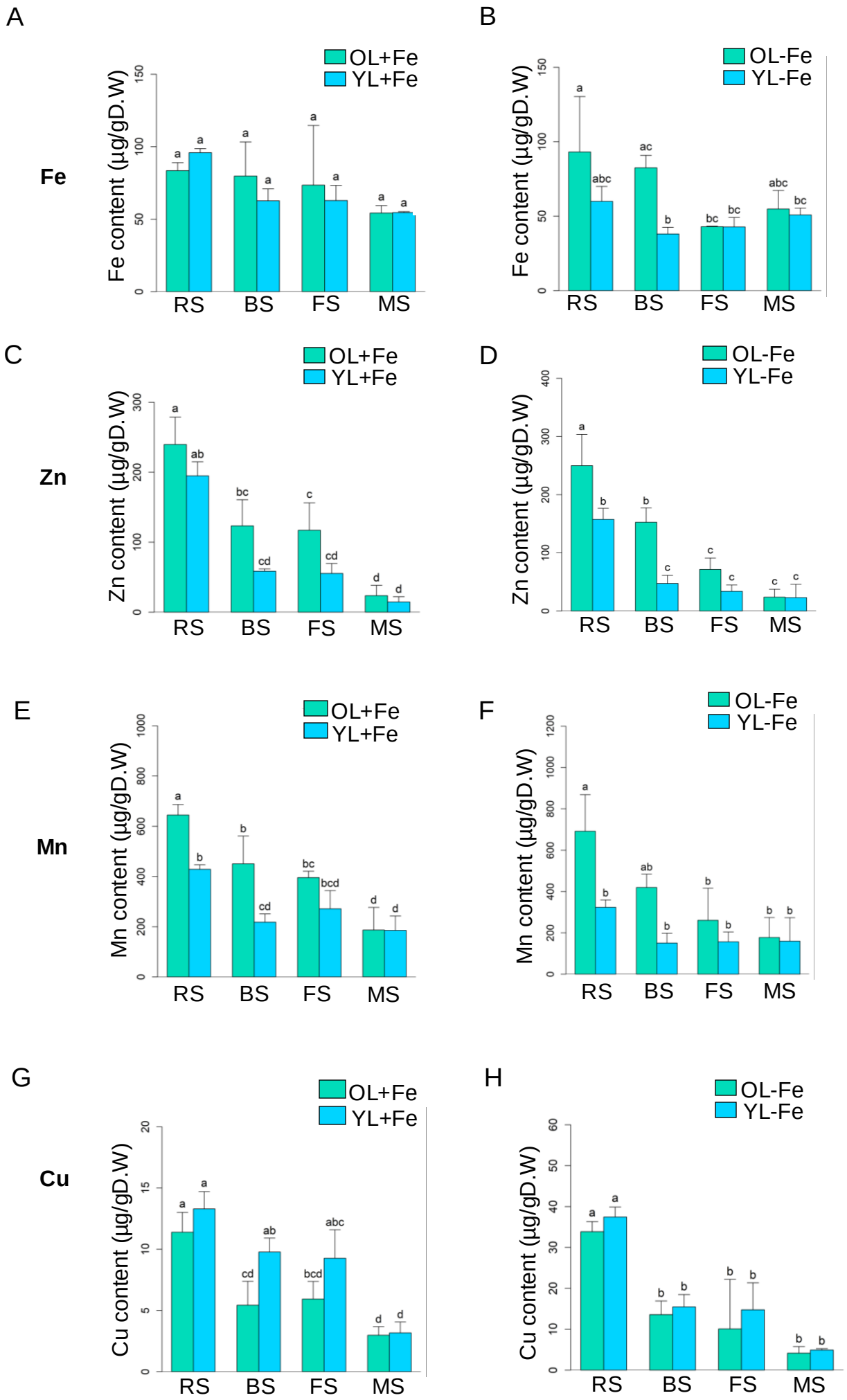
A
B
C
D
E
F
G
H
Fe
Zn
Mn
Cu
OL+Fe
YL+Fe
OL-Fe
YL-Fe
Fe content (µg/gD.W)
Zn content (µg/gD.W)
Mn content (µg/gD.W)
Cu content (µg/gD.W)
RS
BS
FS
MS

Figure S4. Comparison of mineral contents in old (OL) and young (YL) leaves at +Fe and –Fe growth conditions. Fe (A-B), Zn (C-D), Mn (E-F), and Cu (G-H) contents per dry weight (D.W.) in old leaves and young leaves at +Fe or –Fe growth conditions at the growth stages; RS, BS, FS and MS. Plants were exposed to 3 days of +Fe or –Fe before sample collection. Data represents mean of three biological replicates (n = 3). Error bars represent ± SD. Letters on top of each bar show level of significance according to Tukey's HSD test, $p < 0.05$.